8 10 10/6

AEC RESEARCH AND DEVELOPMENT REPORT

Y-1488
Engineering & Equipment

AN ACCELERATION SWITCHING VALVE CONTROL SYSTEM WITH MACHINE TOOL APPLICATION

J. B. Mankin

Y-12 PLANT
Oak Ridge, Tennessee

UNION CARBIDE

UNION CARBIDE CORPORATION
NUCLEAR DIVISION

Operating the

OAK RIDGE GASEOUS DIFFUSION PLANT • OAK RIDGE NATIONAL LABORATORY
OAK RIDGE Y-12 PLANT • PADUCAH GASEOUS DIFFUSION PLANT

For the Atomic Energy Commission
Under U.S. Government Contract W7405 eng 26

DISCLAIMER

Printed in USA. Price $4.00. Available from the Clearinghouse for Federal Scientific and Technical Information, National Bureau of Standards, U.S. Department of Commerce, Springfield, Virginia

Date Issued: September 27, 1965

Report Number Y-1488

Engineering and Equipment
TID-4500 (44th Edition)

UNION CARBIDE CORPORATION
Nuclear Division

Y-12 PLANT

Contract W-7405-eng-26
With the US Atomic Energy Commission

AN ACCELERATION SWITCHING VALVE CONTROL SYSTEM WITH MACHINE TOOL APPLICATION

J. B. Mankin

This report is based on a study by the author as partial fulfillment of requirements for the degree of Master of Science in Electrical Engineering from The University of Tennessee.

Oak Ridge, Tennessee
August 11, 1965

Report Number Y-1488

Engineering and Equipment
TID-4500 (44th Edition)

Distribution:

Ackerson, R. D.	(AFSC)	Keller, C. A.	(AEC-ORO)(4)
Bailey, E. W.		Kite, H. T.	
Ballenger, H. F.	(2)	Lewis, F. O.	(ORGDP)
Bell, B. B.		McLendon, J. D.	
Bernander, N. K.		Mitchel, G. W.	
Briscoe, O. W.		Patton, F. S.	
Burkhart, L. E.		Rader, D. H.	
Center, C. E.	(ORGDP)	Trotter, T. C.	
Christman, A. M.		Waters, J. L.	
Cowen, D. D.	(ORNL)	Whitson, W. K.	
Evans, G. W.		Williams, J. L.	
Harwell, W. L.	(ORGDP)(5)	Winkel, R. A.	(Paducah)
Hemphill, L. F.		Yaggi, W. J.	
Huber, A. P.	(ORGDP)	Zurcher, E.	
Jackson, V. C.		Y-12 Central Files	(5)
Jennings, D. A.		Y-12 Central Files	(Y-12RC)

In addition, this report is distributed in accordance with the category Engineering and Equipment, as given in the "USAEC Standard Distribution Lists for Unclassified Scientific and Technical Reports", TID-4500 (44th Edition), August 1, 1965.

ABSTRACT

With equal emphasis on practice and theory, the application of the acceleration switching valve to machine tool control systems is examined. Utilizing basic hydraulic concepts and electrical analogy techniques, the differential equation describing the acceleration switching valve and its associated load is developed. Root locus techniques are then utilized to snythesize a feedback control system with desirable transient response and steady-state errors. Physical tests are performed to verify all results.

ACKNOWLEDGEMENTS

The author would like to thank the Laboratory Development Department of the Oak Ridge Y-12 Plant, Union Carbide Corporation—Nuclear Division, for permission to conduct this study, and he would like to offer particular thanks to L. E. Burkhart and R. W. Schede for their aid and cooperation. The author would like to express his thanks to V. M. Hovis of the Y-12 Mechanical Development Department who initiated this investigation. Finally, the author would like to express his appreciation to Dr. J. C. Hung for his advice and inspiration.

TABLE OF CONTENTS

LIST OF TABLES

LIST OF FIGURES

FIGURE PAGE

CHAPTER I

INTRODUCTION

Electrohydraulic Control Systems

Ideally the machine tool control system maintains an errorless relationship between the input command and the position of the cutting tool. Although this is impossible in a practical sense, the system error should be well within the tolerance limits. As tolerance limits are lowered in keeping with advancing technology, new and better methods of machine tool control must be developed in conjunction with improvement in the well-established techniques.

Hydraulic systems possess greater stiffness and power-to-weight ratios than do comparable electric actuators. Therefore, superior dynamic response that is less affected by load variations may be obtained with an electrohydraulic system. The hydraulic system is then the best presently available system for precision machining applications.[1, 2]

The Acceleration Switching Valve

The primary element of the electrohydraulic system is the control valve. This system utilizes a relatively new concept in electrohydraulic control known as the acceleration switching valve. Among its advantages over more conventional valves are the following:

1. Greater reliability in the presence of contaminated fluids.
2. Less degradation in performance due to wearing of moving parts.

3. Increased stiffness-to-load variations.

4. Improved resolution.

5. Simplicity of construction.[3, 4]

The acceleration switching valve, therefore, would seem to be ideally suited for reliable, precision machining applications.

The acceleration switching valve is essentially a two-stage, four-way hydraulic valve which may be schematically represented by Figure 1. In construction it is very similar to the more common proportional flow control valve shown in Figure 2, but its principle of operation is quite different. This will be explained in the following paragraphs.

The torque motor and flapper assembly is driven by a square wave of constant repetition rate. The amplitude of the square wave is more than sufficient to saturate the torque motor coils in either direction. For convention in the following discussion, the current that causes Coil A to pull the flapper against Nozzle A will be considered positive. When Nozzle A is sealed, the flow through Orifice A has only one path which is through the "A" control chamber causing the spool to move toward the right. Neglecting transient conditions, there will be a constant flow into the "A" control chamber imparting a constant velocity toward the right to the spool. The flow through the "B" control chamber and the "B" orifice has a common path through the "B" nozzle. When the polarity of the square wave reverses, the spool is caused to move with a constant velocity toward the left by the same physical action with respect to Nozzle B.

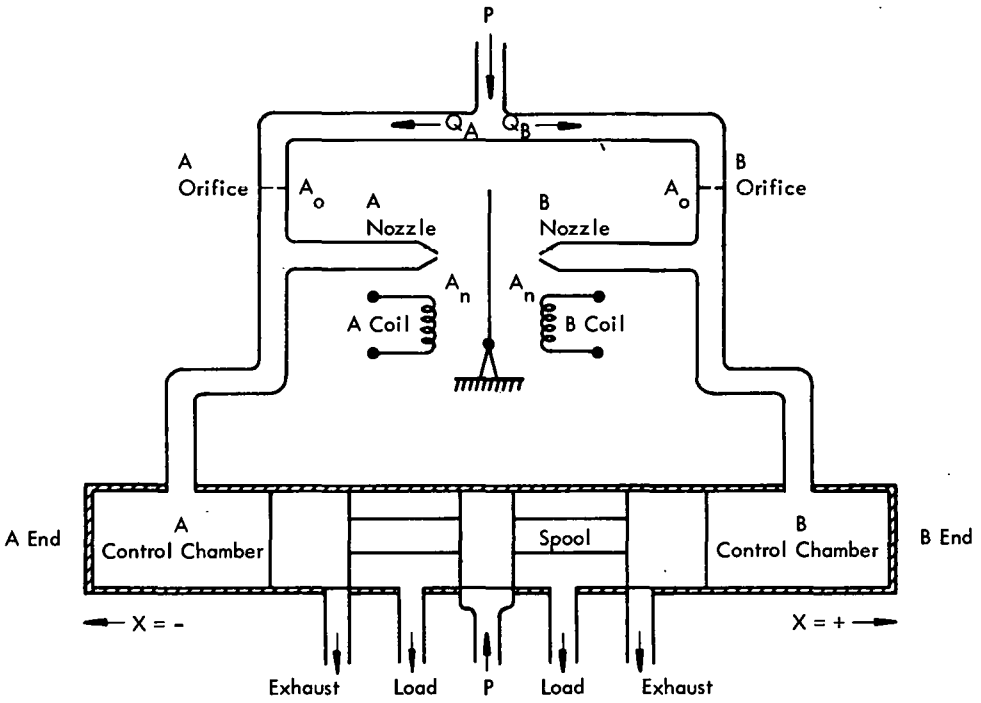

(a) Schematic diagram of the acceleration switching valve

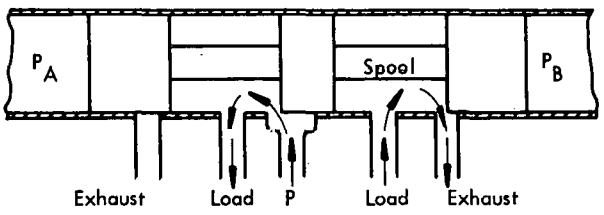

(b) Flow with the valve spool off center

FIGURE 1

THE ACCELERATION SWITCHING VALVE

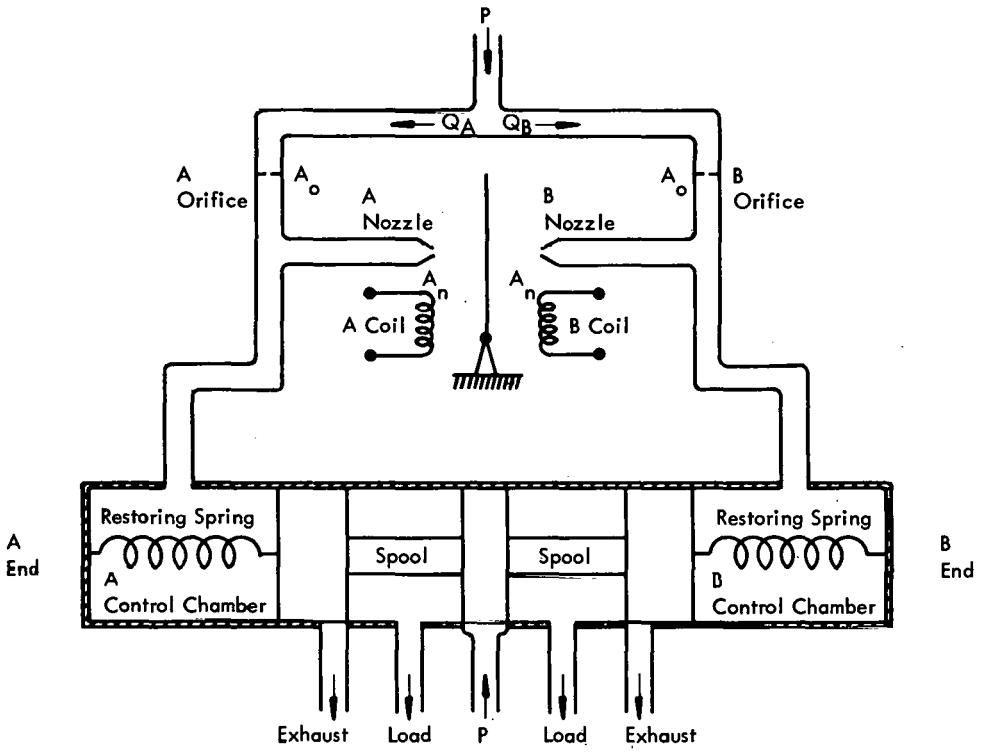

FIGURE 2

SCHEMATIC DIAGRAM OF THE PROPORTIONAL FLOW CONTROL VALVE

The input square wave causes the flapper to alternately seal Nozzles A and B at its repetition rate. This action causes the spool to move alternately right and left rapidly at very small amplitudes. The mixer causes the periods of the positive and negative portions of the square wave to vary in proportion to the error signal. A positive error signal into the mixer causes the positive and negative periods to decrease and increase, respectively, while maintaining a constant total period. The square wave, therefore, has an average DC component proportional to the error signal.

With zero error signal the spool will have a small amplitude variation around its null position, and an unbalanced input will cause the spool to attain an average velocity in the direction commanded by the error signal. Hence, a constant input signal ideally results in a constant velocity, and the spool position is the time integral of the input signal.

As the spool moves from its null position, it uncovers the supply and exhaust ports. Fluid, therefore, flows to the load and returns to the exhaust through matched orifices. If the spool position is held constant, a constant flow will occur through these orifices, and the load position is the time integral of spool position.

Spool velocity rather than position is the control parameter of the acceleration switching valve, and the load position is a double integration of the valve input. In other words, a constant error signal causes the load to attain a constant acceleration, hence the name "acceleration switching valve." The block diagram of the valve is shown in Figure 3.[3, 4, 5]

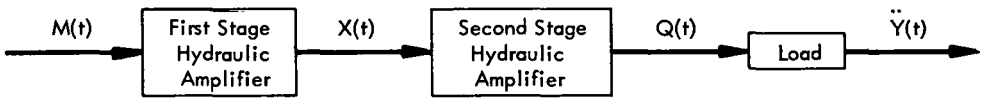

FIGURE 3

BLOCK DIAGRAM OF THE ACCELERATION SWITCHING VALVE AND LOAD

Fixed Components

The block diagram of the basic acceleration switching valve control system is shown in Figure 4. The fixed components of the system are listed below.

1. Linear Variable Differential Transformer (LVDT)

   This device is the feedback element of the system. It consists of a transformer with two secondary coils wound in opposition and mounted in a nonmagnetic case. A moving element of low-loss, high-permeability, magnetic material is suspended within the case. As the moving element moves in either direction, the voltage in one coil increases while it decreases in the other. The summation of the output voltages is proportional to the displacement of the core; and the error signal, in effect, is the difference between the moving core and case positions.[6]

2. Displacement Transducer Amplifier

   This amplifier provides the excitation voltage for the differential transformer primary, and it amplifies the differential signal. The output of this amplifier is a phase detector which converts the signal into a DC signal proportional to the displacement.

3. Mixer

   This element is a differential operational amplifier operating in an open-loop condition. An input signal of approximately ± 2 millivolts is sufficient to saturate the output in a direction depending on the polarity of the input signal. The error signal is impressed on one input

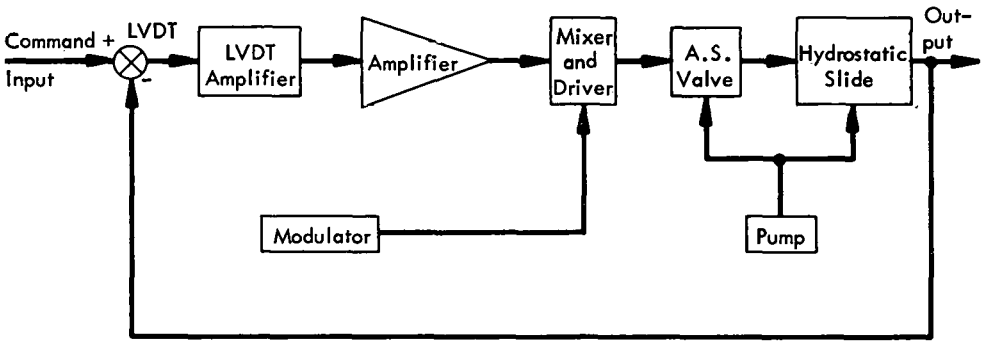

FIGURE 4

THE BLOCK DIAGRAM OF THE BASIC ACCELERATION SWITCHING VALVE CONTROL SYSTEM

grid, and a triangular wave is impressed on the other input grid. The resulting output is the square wave shown in Figure 5. As may be seen, the relationship of the positive and negative periods is proportional to the input error signal.

4. Hydrostatic Slide

This is a comparatively new concept in machine design. The slide is suspended by a high pressure film of oil. It is free to slide in the axis of motion upon application of an extremely small force. Coefficients of friction of less than 4×10^{-6} have been obtained by similar techniques. This, in effect, eliminates static friction and its associated dead band.[7]

Objectives

It is desired to examine the application of the acceleration switching valve to machine tool control systems. Emphasis will be placed on both the practical considerations and theoretical advantages of this valve. This study arises from the necessity of improving automatic machining techniques.

Utilizing basic physical laws, the transfer function of the acceleration switching valve and the hydrostatic slide actuator will be developed. Having developed the transfer function of the fixed components of the system, the feedback control system will be designed to meet specifications. This goal is accomplished by utilizing root locus techniques to achieve proper compensation. It is desired to utilize a logical synthesis procedure rather than the all too common "cut-and-try"

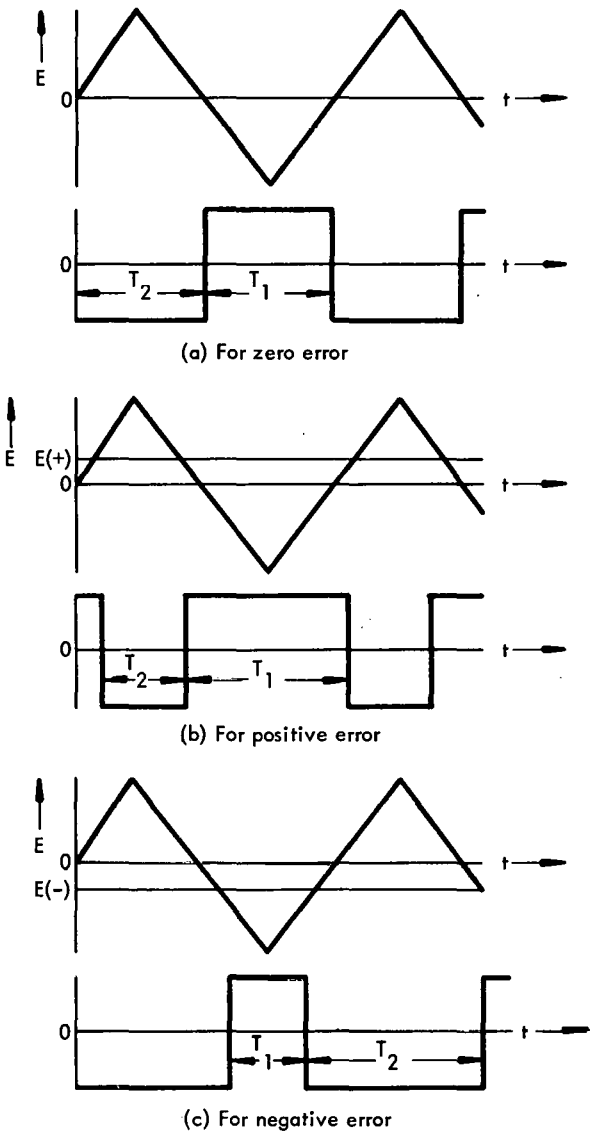

(a) For zero error

(b) For positive error

(c) For negative error

FIGURE 5

MIXER INPUT AND OUTPUT

WAVEFORMS

methods. The final systems will then be built and tested to determine the validity of the analysis and synthesis procedures.

CHAPTER II

BASIC HYDRAULIC CONCEPTS

Electrical Analogies

Electrical analogies is a common technique for describing physical systems. The analogous relationships between electrical and hydraulic quantities are:

1. Current, I, analogous to flow, Q;
2. Voltage, E, analogous to pressure, P; and
3. Conductance, G, analogous to hydraulic conductance, $G = C_D A\sqrt{\frac{2}{\rho}}$.

The relationship between flow and pressure is then given by:

$$Q = G\sqrt{P}. \tag{1}$$

Note that Equation 1 is a nonlinear relationship as opposed to the linear relationship of Ohm's law in the electrical case.

The basic concepts of hydraulic theory have been applied to control valves by Blackburn.[1] Control valves consist of variable and fixed orifices which vary the restriction of flow from a supply to a load as a moving member is positioned by an external signal. It is possible to derive an equivalent circuit for each valve and condition of operation; and a characteristic equation may be derived in terms of P_m, Q_m, and y which are load pressure, load flow, and the input quantity, respectively.

The characteristic equation may be plotted as a family of curves known as $P_m - Q_m$ curves. Due to the inherent nonlinearity of the $P_m - Q_m$ curves, it is

impossible to completely describe the valve with a set of linear differential equations with constant coefficients. The operation of the valve may be approximated by equations obtained from the $P_m - Q_m$ curves by considering some quiescent operating point (usually the origin) and determining the differential coefficients:

$$\left.\frac{\partial Q_m}{\partial y}\right|_{P_m = \text{CONST}}, \quad \left.\frac{\partial Q_m}{\partial P_m}\right|_{y = \text{CONST}}, \text{ and } \left.\frac{\partial P_m}{\partial y}\right|_{Q_m = \text{CONST}}.$$

This procedure is analogous to the small signal analysis of Class A amplifiers, and it is accomplished by considering small perturbations of the input quantity, y. If the analysis is restricted to small perturbations, the control volumes are approximately equal, and the characteristics of flow through the orifices are approximately linear over a restricted range. If this is the case, a linear analysis may be performed with negligible error.[8]

The assumption of small input perturbations is very good in machining applications. It is seldom necessary for the system to respond to large input signals because of the nature of machining operations. The presence of large error signals in precision machine tool control systems normally indicates that the system is already out of tolerance.

Characteristic equations may be derived by the use of certain basic laws. The definition of pressure as a scalar quantity in the hydraulic case corresponds to Kirchhoff's voltage law in the electrical case. Therefore, Kirchhoff's voltage law is also valid for hydraulic circuitry, or

$$\sum_{i=1}^{n} P_i = 0 \tag{2}$$

around a loop. Also, the law of the conservation of mass in the hydraulic case corresponds to Kirchhoff's current law in the electrical case; therefore,

$$\sum_{i=1}^{m} Q_i = 0 \tag{3}$$

at any point. The flow through an orifice is described by the orifice equation (Equation 1). The hydraulic conductance of an orifice varies with the movement of the valve spool, and the characteristics of variation depend upon the design of the valve and must be described in each case.

Hydrodynamic Equations

In a hydraulic control system, the fluid is just as much a part of the system as are the electronic and mechanical components. Since hydraulic fluids exhibit substantial viscous effects, the flow is not completely irrotational. To completely describe the motion of a fluid, a three-dimensional analysis must be used. It is also not possible to assume that flow under rapidly varying conditions is laminar. It may be assumed, however, that the average volume of fluid under turbulent conditions closely approximates the action of the summation of the flow of elementary fluid particles under laminar conditions. The only contribution of turbulence, therefore, is to produce noise. It may be assumed that the flow is quasi-irrotational, laminar, and incompressible with some viscous effect.[1, 11]

The equation describing the flow for a viscous incompressible fluid is the well-known Navier-Stokes equation which is given by:

$$\rho \frac{d\vec{V}}{dt} = - \vec{\nabla} P + \mu \nabla^2 \vec{V} + \vec{F}, \tag{4}$$

where:

$\rho \frac{d\vec{V}}{dt}$ represents the force per unit volume due to acceleration,

$\vec{\nabla} P$ the pressure force per unit volume,

$\mu \nabla^2 \vec{V}$ the viscous force per unit volume, and

$\vec{F}$ the external force per unit volume acting on the fluid.[9, 10, 12, 13]

If Equation 4 is applied to the elementary fluid particle shown in Figure 6, it becomes:

$$\rho \frac{d\vec{V}}{dt} = - \vec{i} \frac{\partial P}{\partial x} - \vec{j} \frac{\partial P}{\partial y} - \vec{k} \frac{\partial P}{\partial y} + \mu \left(\frac{\partial^2 \vec{V}}{\partial x^2} + \frac{\partial^2 \vec{V}}{\partial y^2} + \frac{\partial^2 \vec{V}}{\partial z^2} \right) + \Sigma \vec{F}. \tag{5}$$

If u, v, and w are the components of velocity in the x, y, and z directions, respectively, it should be noted that they are not only functions of the coordinates of the point (x, y, z) but also of time, t. The term on the left-hand side of Equation 5 therefore becomes:

$$\rho \frac{d\vec{V}}{dt} = \rho \frac{d^2\vec{r}}{dt^2} = \rho \left[\vec{i} \left(\frac{\partial u}{\partial t} + \frac{\partial u}{\partial x} \frac{\partial x}{\partial t} + \frac{\partial u}{\partial y} \frac{\partial y}{\partial t} + \frac{\partial u}{\partial z} \frac{\partial z}{\partial t} \right) + \vec{j} \left(\frac{\partial v}{\partial t} + \frac{\partial v}{\partial x} \frac{\partial x}{\partial t} + \frac{\partial v}{\partial y} \frac{\partial y}{\partial t} + \frac{\partial v}{\partial z} \frac{\partial z}{\partial t} \right) + \vec{k} \left(\frac{\partial w}{\partial t} + \frac{\partial w}{\partial x} \frac{\partial x}{\partial t} + \frac{\partial w}{\partial y} \frac{\partial y}{\partial t} + \frac{\partial w}{\partial z} \frac{\partial z}{\partial t} \right) \right],^{10} \tag{6}$$

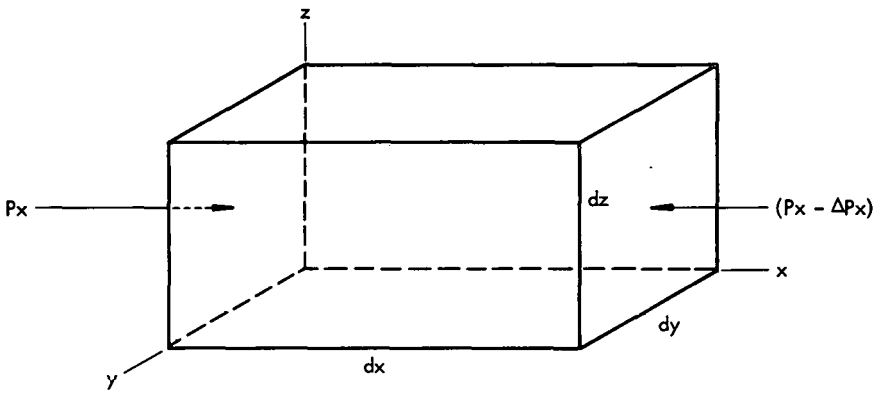

FIGURE 6

INCREMENTAL ELEMENT OF A FLUID

where "r" is the path traversed by the incremental fluid element.

The Navier-Stokes equations for the x, y, and z directions therefore become:

$$\rho\left(\frac{\partial u}{\partial t}+\frac{\partial u}{\partial x}\frac{\partial x}{\partial t}+\frac{\partial u}{\partial y}\frac{\partial y}{\partial t}+\frac{\partial u}{\partial z}\frac{\partial z}{\partial t}\right)=-\frac{\partial P}{\partial x}+\mu\left(\frac{\partial^2 u}{\partial x^2}+\frac{\partial^2 u}{\partial y^2}+\frac{\partial^2 u}{\partial z^2}\right)+F_x, \quad (7)$$

$$\rho\left(\frac{\partial v}{\partial t}+\frac{\partial v}{\partial x}\frac{\partial x}{\partial t}+\frac{\partial v}{\partial y}\frac{\partial y}{\partial t}+\frac{\partial v}{\partial z}\frac{\partial z}{\partial t}\right)=-\frac{\partial P}{\partial y}+\mu\left(\frac{\partial^2 v}{\partial x^2}+\frac{\partial^2 v}{\partial y^2}+\frac{\partial^2 v}{\partial z^2}\right)+F_y, \text{and} \quad (8)$$

$$\rho\left(\frac{\partial w}{\partial t}+\frac{\partial w}{\partial x}\frac{\partial z}{\partial t}+\frac{\partial w}{\partial y}\frac{\partial y}{\partial t}+\frac{\partial w}{\partial z}\frac{\partial z}{\partial t}\right)=-\frac{\partial P}{\partial z}+\mu\left(\frac{\partial^2 w}{\partial x^2}+\frac{\partial^2 w}{\partial y^2}+\frac{\partial^2 w}{\partial z^2}\right)+F_z.^{13} \quad (9)$$

If the volume of fluid is examined on a macroscopic scale, the forces in the "y" direction may be considered to be equalized due to the fact that the fluid is enclosed in small tubing; therefore, $F_y = 0$. There is some differential in body force in the "z" direction due to the difference in head, but since the diameter of the tubing is small, this may be considered to be negligible; therefore, $F_z \simeq 0$. The pressure acting on the fluid is normal to the surface of the fluid at all points around the tube. Since there are no pressure sources or sinks around the circumference, $\partial P/\partial y = \partial P/\partial z = 0$. There is also no resultant average velocity or acceleration in the "y" and "z" directions on a macroscopic scale, therefore, $v = w = 0$. This is not quite true at a point due to turbulence and rotational properties. In light of the above, all terms in Equations 8 and 9 are zero, and Equation 7 becomes:

$$\rho\left(\frac{\partial u}{\partial t}+\frac{\partial u}{\partial x}\frac{\partial x}{\partial t}\right)=-\frac{\partial P}{\partial x}+\mu\left(\frac{\partial^2 u}{\partial x^2}+\frac{\partial^2 u}{\partial y^2}+\frac{\partial^2 u}{\partial z^2}\right)+F_x. \tag{10}$$

Equations 7 through 10 result from the Navier-Stokes equations for a viscous, incompressible fluid. Although a hydraulic fluid is not quite incompressible, the Navier-Stokes equations for a compressible fluid are quite complicated,[14] so the assumption of incompressibility is made for the sake of simplicity at little sacrifice in accuracy. Compressibility will be examined later by assuming the effect of compressibility to behave as a linear spring.[1]

Throughout tubing of the same cross-sectional area, there can be no change in velocity in the "x" direction due to the principle of continuity. Equation 10, therefore, becomes:

$$\rho\frac{du}{dt}=-\frac{\partial P}{\partial x}+\mu\left(\frac{\partial^2 u}{\partial y^2}+\frac{\partial^2 u}{\partial z^2}\right)+F_x. \tag{11}$$

The macroscopic volume of fluid is actually similar to Figure 7. If the transformation is made:

$$x = x,$$

$$y = r\cos\theta, \text{ and}$$

$$z = r\sin\theta, \tag{12}$$

Equation 11 becomes:

$$\rho\frac{du}{dt}=-\frac{\partial P}{\partial x}+\mu\left[\frac{1}{r}\frac{\partial}{\partial r}\left(r\frac{du}{dr}\right)+\frac{1}{r^2}\frac{\partial^2 u}{\partial\theta^2}\right]+F_x. \tag{13}$$

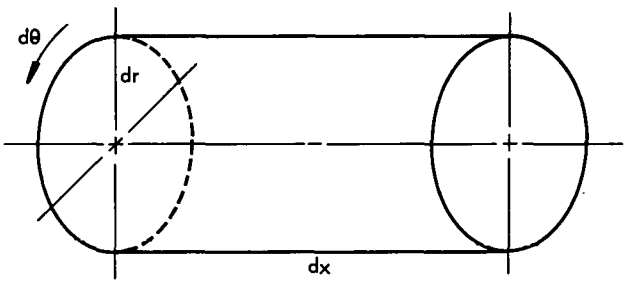

FIGURE 7

VOLUME OF A FLUID IN A TUBE

Remembering the assumption that the flow approximates the total effect of laminar flow, it may be assumed that the velocity does not change with respect to θ, and Equation 13 becomes:

$$\rho \frac{du}{dt} = - \frac{\partial P}{\partial x} + \mu \left(\frac{1}{r} \frac{\partial u}{\partial r} + \frac{\partial^2 u}{\partial r^2} \right) + F_x .^{13} \tag{14}$$

A rigorous analysis of Equation 14 necessitates determining the velocity profile of the fluid in the cross section of the pipe which is beyond the scope of this thesis. The effect of fluid viscosity, however, may be approximately determined by the Hagen-Poiseuille relationship which is given by:

$$1/2 \, u \, \pi \, r^2 = \frac{\pi r^4 \Delta P}{8 \mu L} .^{13} \tag{15}$$

Solving Equation 15 for the shearing force per unit volume results in:

$$\frac{\Delta P}{L} = \frac{F}{V} = \frac{4 \mu}{r^2} u. \tag{16}$$

This relationship is equivalent to the second term on the right-hand side of Equation 14; therefore, Equation 14 becomes:

$$\rho \frac{du}{dt} = - \frac{\partial P}{\partial x} + \frac{4 \mu}{r^2} u + F_x, \tag{17}$$

which, in turn, becomes:

$$\rho \frac{d^2 x}{dt^2} = - \frac{\partial P}{\partial x} + \frac{4 \mu}{r^2} \frac{dx}{dt} + F_x . \tag{18}$$

Each term in Equation 18 is expressed in pounds per cubic inch.

It should be noted that the pressure decreases as "x" increases which means that it is a pressure drop. The velocity is a maximum at the centerline and zero at the pipe boundary. Considering the source of supply pressure as the origin, it should be observed that the body forces are those exerted by the spool and its reaction forces. This force is in a direction opposing the flow. Considering the above, the sign of the right-hand side of Equation 18 should be reversed. Also, over the full length of the tubing, $\partial P/\partial x$ becomes $\Delta P/L$. Equation 18 then becomes:

$$\frac{\Delta P}{L} = \rho \frac{d^2x}{dt^2} + \frac{4\mu}{r^2}\frac{dx}{dt} + \frac{\Sigma F_m}{V}. \qquad (19)$$

The equation for the force balance may be found by multiplying Equation 19 by the fluid volume yielding:

$$A \Delta P = A L \rho \frac{d^2x}{dt^2} + 4 \pi L \mu \frac{dx}{dt} + \Sigma F_m, \qquad (20)$$

where:

ΔP represents the pressure drop across the fluid volume,

L the effective length of the tubing,

ρ the mass density of the fluid,

μ the viscosity of the fluid,

r the effective radius of the tubing,

F_m the reaction forces of the spool, and

V the total volume of entrained fluid.

Equation 20 is the force balance on the fluid considering the fluid mass as a free-body diagram.

CHAPTER III

EQUATIONS OF MOTION

First-Stage Hydraulic Amplifier

Electrical Analogy. The electrical analog of the acceleration switching valve at the switching frequency is shown in Figure 8. The pulse width type of modulation causes the torque motor to act as a polarity-sensitive relay. Effectively, this relay alternately switches the supply pressure from the "A" chamber to the "B" chamber and vice versa in the hydraulic circuit.

The electrical analog of the acceleration switching valve is no longer the circuit of Figure 8 at the control frequencies. Control frequencies are defined as frequencies within the spectrum of the closed-loop system, and it is assumed that the switching frequency is well outside this spectrum. Within this range of frequencies the effect of switching is to make it appear as if the flapper maintains an average position somewhere between Nozzles A and B, thereby varying the hydraulic conductance of the nozzles.

The electrical analog of the first stage of the acceleration switching valve is, therefore, a full bridge with two variable arms. This relationship may be seen by an examination of the equations of flow through the nozzles. During any period of time the flow through Nozzle A is described by:

$$Q_{NA} = C_D A_{NA_{eff}} \sqrt{\frac{2 \Delta P}{\rho}}. \tag{21}$$

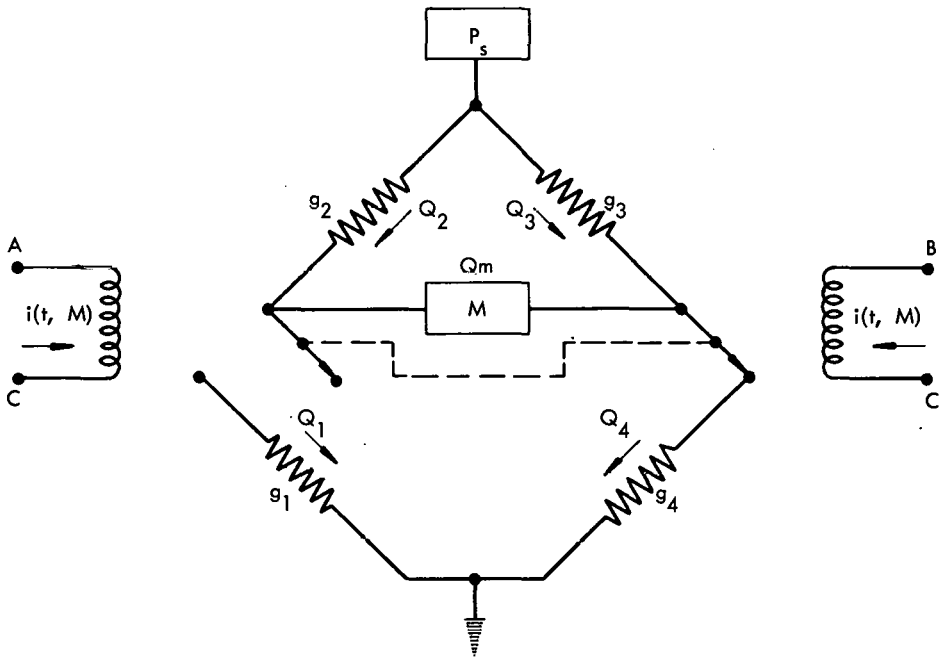

FIGURE 8

ELECTRICAL ANALOG OF AN ACCELERATION SWITCHING VALVE AT MODULATION FREQUENCY

During the positive period of the input square wave, $A_{NA_{eff}} = 0$, and during the negative period, $A_{NA_{eff}} = A_{NA}$. The effect during the total period with $m(t) = 0$ ($T_1 = T_2$) is to make the equation of flow through Nozzle A become:

$$Q_{NA} = \frac{C_D A_{NA}}{2} \sqrt{\frac{2 \Delta P}{\rho}} . \tag{22}$$

The effect of this orifice at the control frequencies is proportional to the relative amount of time the nozzle is closed. In other words, it is directly proportional to $m(t)$. If $m(t) = +1$, the signal is fully positive, and Nozzle A is completely closed. If $m(t) = -1$, the signal is fully negative, and the nozzle is opened at all times. Q_{NA} is related to $m(t)$, therefore, by the following relations:

$$m(t) = +1 \qquad Q_{NA} = 0, \tag{23-a}$$

$$m(t) = 0 \qquad Q_{NA} = \frac{C_D A_{NA}}{2} \sqrt{\frac{2 \Delta P}{\rho}}, \text{ and} \tag{23-b}$$

$$m(t) = -1 \qquad Q_{NA} = C_D A_{NA} \sqrt{\frac{2 \Delta P}{\rho}} . \tag{23-c}$$

Since Q_{NA} is linearly related to $m(t)$, the effective hydraulic conductance of Nozzle A at the control frequencies is given by:

$$g_{NA} = (1 - m(t)) \frac{C_D A_{NA}}{2} \sqrt{\frac{2}{\rho}} . \tag{24}$$

Similarly, the effective hydraulic conductance of Nozzle B is given by:

$$g_{NB} = (1 + m(t)) \frac{C_D A_{NB}}{2} \sqrt{\frac{2}{\rho}} . \tag{25}$$

Equations 24 and 25 are the equations describing the variable arms of the bridge. The analogous circuit for the first-stage hydraulic amplifier is found in Figure 9.[1]

$P_m - Q_m$ Curves.

Derivation. The $P_m - Q_m$ curves may now be derived in terms of the input variable $m(t)$. Using Kirchhoff's laws, the following circuit equations may be obtained from Figure 9:

$$P_s - P_2 - P_1 = 0, \tag{26-a}$$

$$P_s - P_2 - P_m - P_4 = 0, \tag{26-b}$$

$$Q_2 - Q_m - Q_1 = 0, \tag{26-c}$$

$$Q_3 + Q_m - Q_4 = 0, \tag{26-d}$$

$$Q_1 = g_1 \sqrt{P_1}, \tag{26-e}$$

$$Q_2 = g_2 \sqrt{P_2}, \tag{26-f}$$

$$Q_3 = g_3 \sqrt{P_3}, \text{ and} \tag{26-g}$$

$$Q_4 = g_4 \sqrt{P_4}. \tag{26-h}$$

Combining Equations 26-a and 26-b yields:

$$P_s - (P_s - P_1) - P_m - P_4 = 0,$$

or

$$P_m = P_1 - P_4. \tag{27}$$

Also from Equations 26-a and 26-e we have:

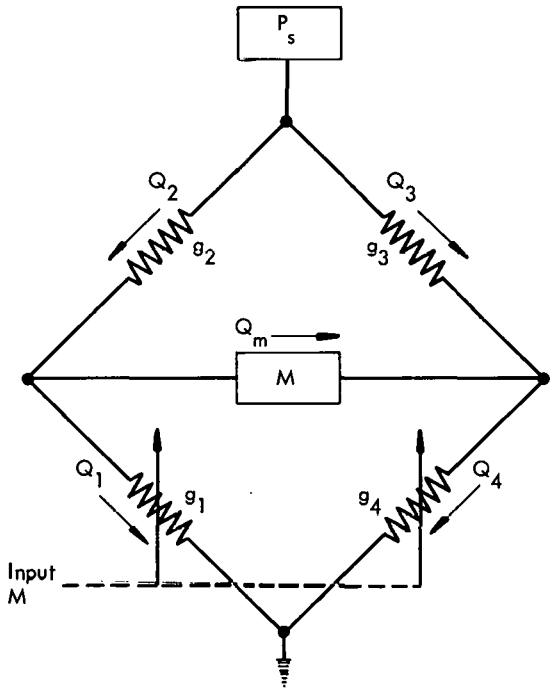

$g_1 = g_{NA}$

$g_2 = g_{OA}$

$g_3 = g_{OB}$

$g_4 = g_{NB}$

FIGURE 9

ELECTRICAL ANALOG OF THE FIRST-STAGE HYDRAULIC AMPLIFIER AT CONTROL FREQUENCIES

$$P_1 = P_s - \frac{Q_2^2}{g_2^2}, \tag{28}$$

and from Equation 26-c,

$$Q_2 = Q_m + Q_1. \tag{29}$$

If we combine Equation 27, 28, and 29, we have:

$$P_1 = P_s - \frac{(Q_m + Q_1)^2}{g_2^2}, \text{ or}$$

$$= P_s - \frac{1}{g_2^2}(Q_m^2 + 2 Q_1 Q_m + Q_1^2), \tag{30}$$

which becomes:

$$P_1 + \frac{2g_1\sqrt{P_1}}{g_2^2} Q_m + \frac{g_1^2 P_1}{g_2^2} = P_s - \frac{Q_m^2}{g_2^2}. \tag{31}$$

Finally, combining Equations 24 and 31 yields:

$$P_1 + (1 - M)\frac{A_1\sqrt{P_1}}{C_D A_2^2\sqrt{\frac{2}{\rho}}} Q_m + (1 - M)^2 \frac{A_1^2 P_1}{4 A_2^2} = P_s - \frac{Q_m^2}{g_2^2}. \tag{32}$$

In a similar manner, combining Equations 26-b and 26-d yields:

$$P_4 = P_s - \frac{(Q_4 - Q_m)^2}{g_3^2}, \tag{33}$$

which becomes:

$$P_4 + \frac{g_4^2}{g_3^2} P_4 - \frac{2g_4}{g_3^2}\sqrt{P_4}\, Q_m = P_s - \frac{Q_m^2}{g_3^2}. \tag{34}$$

Combining Equations 33 and 34 results in:

$$P_4 - (1 + M) \frac{A_4 \sqrt{P_4}}{C_D A_3^2 \sqrt{\frac{2}{\rho}}} Q_m + (1 + M)^2 \frac{A_4^2}{4 A_3^2} P_4 = P_s - \frac{Q_m^2}{g_3^2}. \quad (35)$$

If we now combine Equations 27, 32, and 35, the solutions of P_m, Q_m, and $m(t)$ may be obtained. Notice, however, that there are three equations and five unknowns. Their solution also involves small differences between large numbers. This difficult situation may be overcome by solving these equations for a family of curves on a digital computer (see Appendix B, Page 100). From this solution the $P_m - Q_m$ characteristic curves for the first-stage hydraulic amplifier may be obtained. This solution is shown in Figure 10 while the region around the origin has been expanded in Figure 11.

Differential Coefficients and Transfer Function. Referring to Figure 1 (Chapter I, Page 3) and utilizing the work of Shearer,[8] it is found that the average spool velocity is given by:

$$A_m \Delta (DX) = \left|K_m\right| \Delta M - \left|C_m\right| \Delta P_m - \Delta Q_{c_m} - \frac{V_i}{2\beta} \Delta (DP_m),^{15} \quad (36)$$

where "Δ" indicates a small perturbation from the steady state. Due to the close tolerances held in machining, the leakage around the spool is considered to be negligible. The pressure drop across the spool is balanced by the reaction forces on the spool; therefore,

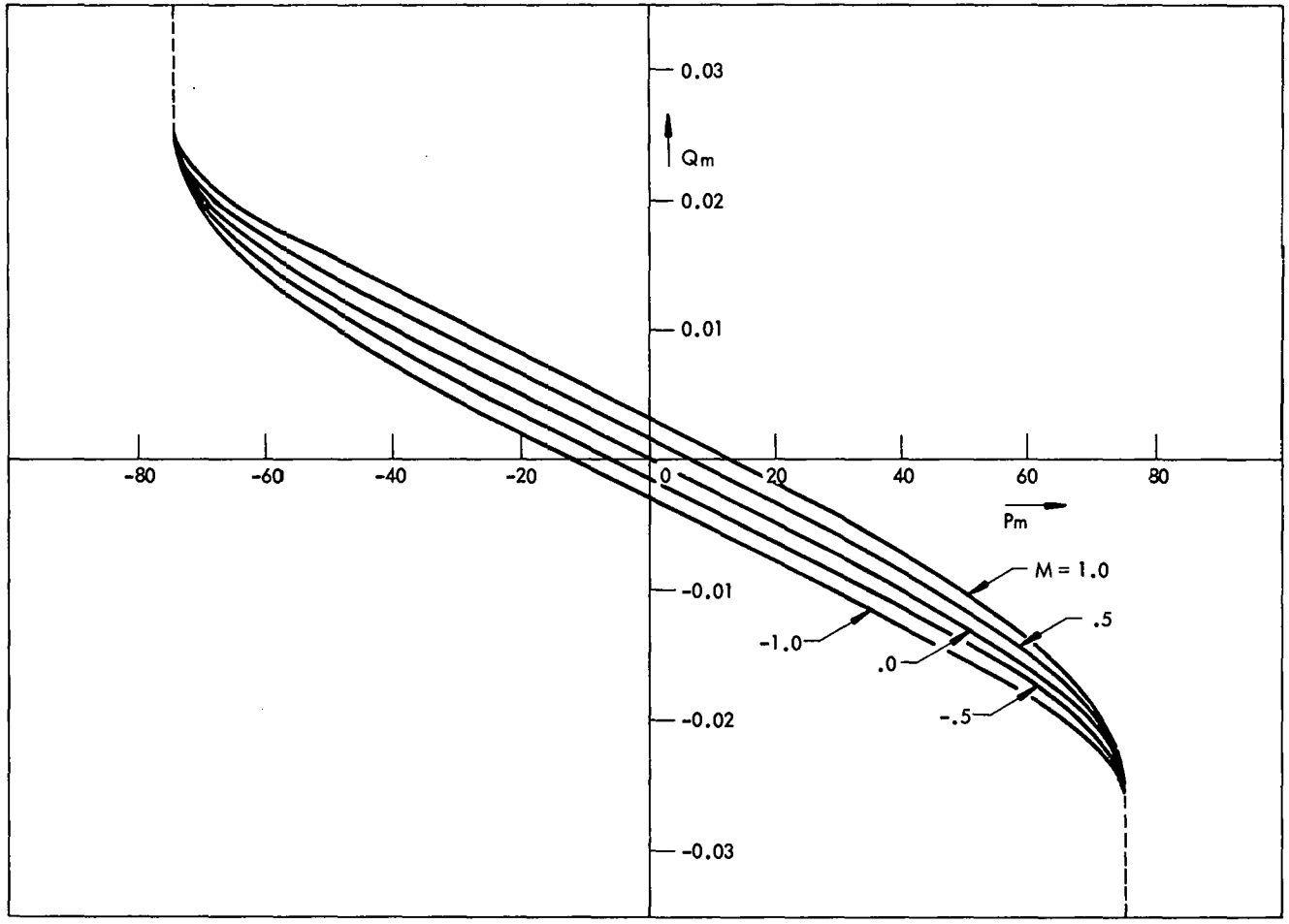

FIGURE 10

CHARACTERISTIC $P_m - Q_m$ CURVES OF FIRST-STAGE HYDRAULIC AMPLIFIER FOR CONSTANT VALUES OF MODULATION INDEX

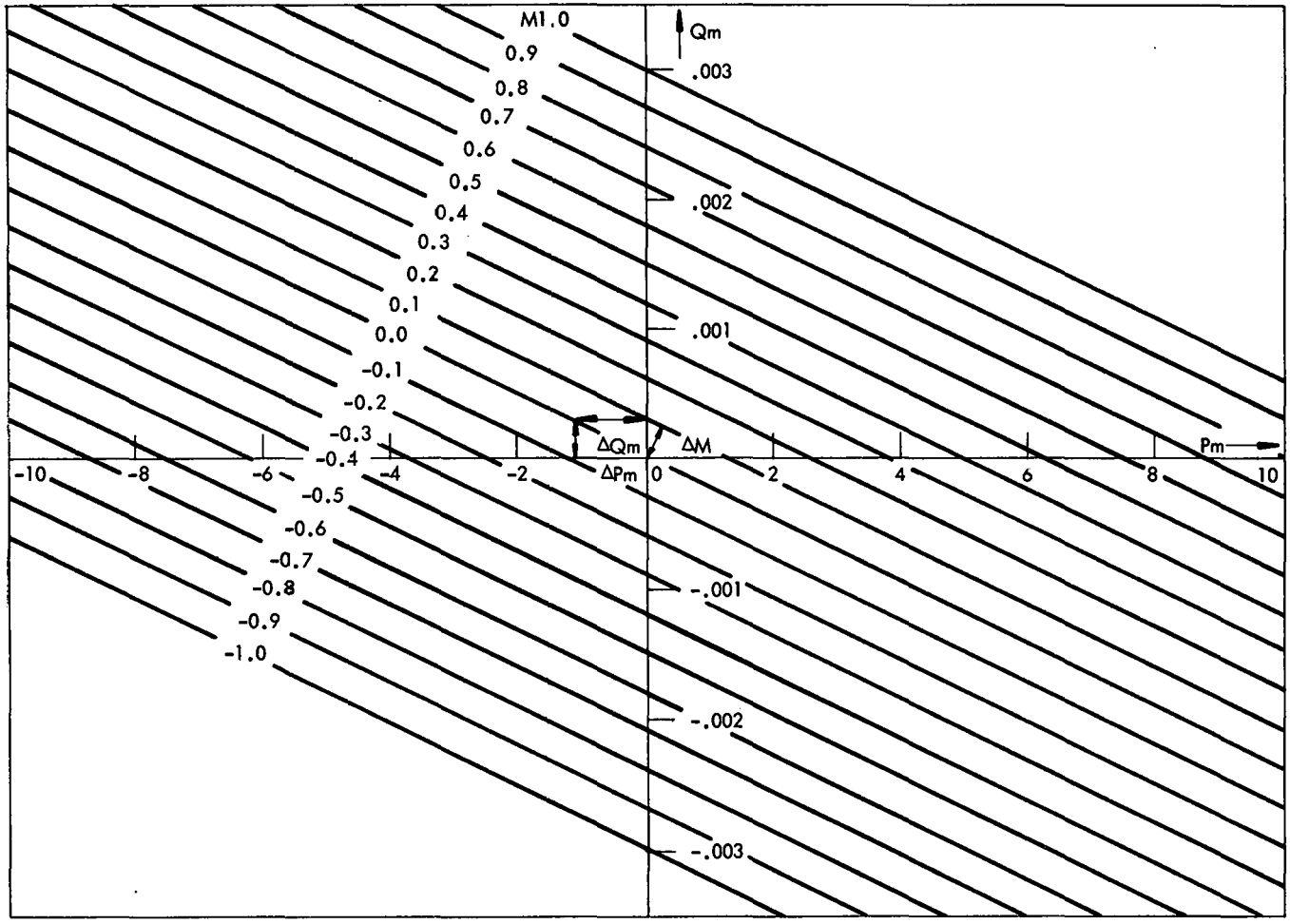

FIGURE 11

CHARACTERISTIC P_m-Q_m CURVES WITH THE REGION AROUND THE ORIGIN EXPANDED

$$P_m = \frac{\Sigma F_{spool}}{A_s} . \tag{37}$$

The coefficients K_m and C_m may be found from the $P_m - Q_m$ characteristic curves.

Referring to Figure 11:

$$\left.\frac{\partial Q_m}{\partial M}\right|_{P_m = CONST} = \lim_{\Delta M \to 0} \left.\frac{\Delta Q_m}{\Delta M}\right|_{P_m = CONST}, \tag{38}$$

$$\simeq \left.\frac{\Delta Q_m}{\Delta M}\right|_{P_m = CONST},$$

$$\simeq \frac{0.0003 - 0.0000}{0.1 - 0.0},$$

$$\simeq 3 \times 10^{-3} \ \frac{In^3/Sec}{100\% \text{ Unbalance}} .$$

$$\left.\frac{\partial Q_m}{\partial P_m}\right|_{M = CONST} = \lim_{\Delta P_m \to 0} \left.\frac{\Delta Q_m}{\Delta P_m}\right|_{M = CONST}, \tag{39}$$

$$\simeq \left.\frac{\Delta Q_m}{\Delta P_m}\right|_{M = CONST},$$

$$\simeq \frac{0.0003 - 0.0000}{-1.25 - 0.00},$$

$$\simeq -2.4 \times 10^{-4} \ \frac{In^3/Sec}{Lbs/In^2} .$$

The reaction forces acting on the valve may be divided into the following:

F_1 the flow reaction forces,

F_2 the force due to the viscous friction of the spool and the fluid, and

F_3 the inertia forces of the spool and fluid.

The flow reaction force is given by the following equation:

$$F_1 = 2\,(2C_D\, d_c\, P_D \cos\theta)\, x + (C_D\, d_c \sqrt{2P_D\, \rho}\, L_m) \frac{dx}{dt}.^{1,11} \qquad (40)$$

Since in the acceleration switching valve the inward flow by the spool has the same path length as the outward flow by the spool, the algebraic sum of the damping lengths, L_m, is zero.

To maintain the system approximately linear, consider that the spool is displaced from its null position to a small input displacement of x. The load presented by the second-stage hydraulic amplifier consists of the supply and return orifices and the slide in series. Since the slide motion may be maintained by a very small force, almost all of the pressure drop appears across the supply and return orifices. Since these are matched orifices, one-half of the supply pressure will be dropped across each one. This condition is similar to the voltage relationships in a simple series circuit composed of resistances and an inductance. The flow reaction forces are, therefore, given by:

$$F_1 = 2\left[2\,(0.6)(0.05)(250)\cos 69^\circ\right] x, \text{ or}$$

$$= (10.7 \text{ lbs/in})\, x. \qquad (41)$$

According to Blackburn,[1] the equation for the flow reaction force is somewhat nonlinear especially in the small input perturbation range. Its deviation

from linearity, however, is slight, and Equation 41 may be assumed to hold with little error. This equation points out the fact that the separate hydraulic stages are not completely isolated from each other.

The force due to the viscous friction of the fluid may be found from Equation 20 (Chapter II, Page 21); therefore, the total viscous force including both the spool and the fluid is given by:

$$F_2 = \mu \frac{A_m}{h_m} \frac{dx}{dt} + \mu \frac{V_t}{r_t^2} \frac{dx}{dt}.^{16} \tag{42}$$

The first term on the right-hand side of Equation 42 is due to the shearing stress in the fluid between the spool and its bushing caused by the movement of the spool, and the second term on the right-hand side is the shearing stress in the tubing fluid. This relationship is given by:

$$F_2 = 3.7 \times 10^{-6} \frac{\text{lb-sec}}{\text{in}^2} \left(\frac{0.32}{0.0001} \frac{\text{in}^2}{\text{in}} + \frac{0.339}{0.03} \frac{\text{in}^2}{\text{in}} \right) \frac{dx}{dt} +$$

$$4\pi (4.3)\ \text{in} \left(3.7 \times 10^{-6} \frac{\text{lb-sec}}{\text{in}^2} \right) \frac{dx}{dt}, \text{ or} \tag{43}$$

$$= 3.7 \times 10^{-6} \frac{\text{lb-sec}}{\text{in}^2} \ (3200\ \text{in} + 11.3\ \text{in} + 54\ \text{in}) \frac{dx}{dt}, \text{ or}$$

$$= 3.7 \times 10^{-6} \frac{\text{lb-sec}}{\text{in}^2} \ (3265.3\ \text{in}) \frac{dx}{dt}, \text{ or}$$

$$= \left(0.0121 \frac{\text{lb-sec}}{\text{in}} \right) \frac{dx}{dt}.$$

The initial force due to the fluid may be found from Equation 20 (Chapter II, Page 21); therefore, the total inertial force is given by:

$$F_3 = M_m \frac{d^2x}{dt^2} + V_t \rho \frac{d^2x}{dt^2}. \tag{44}$$

When the numerical values are substituted, Equation 44 becomes:

$$F_3 = \left[0.0002 \frac{\text{lb-sec}^2}{\text{in}} + 2\,(2.94 \times 10^{-2}\ \text{in}^3)\left(7.95 \times 10^{-5} \frac{\text{lb-sec}^2}{\text{in}^4}\right)\right] \frac{d^2x}{dt^2}, \text{ or} \tag{45}$$

$$= \left(0.0002 \frac{\text{lb-sec}^2}{\text{in}} + 0.00000468 \frac{\text{lb-sec}^2}{\text{in}}\right) \frac{d^2x}{dt^2}, \text{ or}$$

$$- \left(0.000205 \frac{\text{lb-sec}^2}{\text{in}}\right) \frac{d^2x}{dt^2}.$$

Combining Equations 41, 43, and 45 gives the total summation of forces on the valve spool which is:

$$\Sigma F_s = \left(0.000205 \frac{\text{lb-sec}^2}{\text{in}}\right) \frac{d^2x}{dt^2} + \left(0.0121 \frac{\text{lb-sec}}{\text{in}}\right) \frac{dx}{dt} + \left(10.7 \frac{\text{lbs}}{\text{in}}\right) x. \tag{46}$$

Now substituting Equations 37, 38, 39, and 46 into Equation 36 results in:

$$0.0314\ \text{in}^3 \frac{dx}{dt} = 3 \times 10^{-3} \frac{\text{in}^3/\text{sec}}{\text{UNB}}\, m(t) - 2.4 \times 10^{-4} \frac{\text{in}^3/\text{sec}}{\text{lbs/in}^2} \left[\left(0.000205 \frac{\text{lb-sec}^2}{\text{in}} \right) \frac{d^2x}{dt^2} + \left(0.0121 \frac{\text{lb-sec}}{\text{in}} \right) \frac{dx}{dt} + (10.7\ \text{in})\, x \right] \frac{1}{0.0314\ \text{in}^2} -$$

$$1/2 \left(\frac{2.94 \times 10^{-3}\ \text{in}^3}{2.5 \times 10^5\ \text{lbs/in}^2} \right) \frac{d}{dt} \left[\left(0.000205 \frac{\text{lb-sec}^2}{\text{in}} \right) \frac{d^2x}{dt^2} + \left(0.0121 \frac{\text{lb-sec}}{\text{in}} \right) \frac{dx}{dt} + \left(10.7 \frac{\text{lbs}}{\text{in}} \right) x \right] \frac{1}{0.0314\ \text{in}^2}. \qquad (47)$$

Now assuming zero initial conditions and taking the Laplace transform of Equation 47 yields:

$$0.0314\ \text{in}^2\, s\, X(s) - 3 \times 10^{-3} \frac{\text{in}^3/\text{sec}}{\text{UNB}} -$$

$$7.65 \times 10^{-3} \frac{\text{in}^3/\text{sec}}{\text{lb}} \left[0.000205 \frac{\text{lb-sec}^2}{\text{in}}\, s^2 X(s) + 0.0121 \frac{\text{lb-sec}}{\text{in}}\, s\, X(s) + 10.7 \frac{\text{lbs}}{\text{in}}\, X(s) \right] -$$

$$1.87 \times 10^{-6} \frac{\text{in}^3}{\text{lb}} \left[0.000205 \frac{\text{lb-sec}^2}{\text{in}}\, s^2 X(s) + 0.0121 \frac{\text{lb-sec}}{\text{in}}\, s\, X(s) + 10.7 \frac{\text{lbs}}{\text{in}}\, X(s) \right]. \qquad (48)$$

Dividing each side by the piston area this becomes:

$$s\,X(s) = 9.56 \times 10^{-2}\ \frac{in/sec}{UNB}\ M(s) -$$

$$0.244\ \frac{in/sec}{lb}\left[0.000205\ \frac{lb\text{-}sec^2}{in}\ s^2\,X(s) +\right.$$

$$\left.0.0121\ \frac{lb\text{-}sec}{in}\ s\,X(s) + 10.7\ \frac{lbs}{in}\ X(s)\right] -$$

$$5.95 \times 10^{-5}\ \frac{in}{lb}\ s\left[0.000205\ \frac{lb\text{-}sec^2}{in}\ s^2\,X(s) + 0.0121\ \frac{lb\text{-}sec}{in}\ s\,X(s) +\right.$$

$$\left.10.7\ \frac{lbs}{in}\ X(s)\right]. \qquad (49)$$

Now, collecting terms this becomes:

$$X(s)\ \ (1.19 \times 10^{-8}\ s^3 + 4.95 \times 10^{-5}\ s^2 + 1.0096\ s +$$

$$2.62) = 9.56 \times 10^{-2}\ \frac{in/sec}{UNB}\ M(s), \qquad (50)$$

and the transfer function for the first-stage hydraulic amplifier is:

$$\frac{X(s)}{M(s)} = \frac{9.56 \times 10^{-2}\ in/sec/UNB}{1.19 \times 10^{-8}\ s^3 + 4.95 \times 10^{-5}\ s^2 + 1.0096\,s + 2.62}. \qquad (51)$$

The denominator of the right-hand side has a root at $s = -2.6$, while the other roots are at $s = (-2.09 \pm j\ 9.0)\ 10^3$ which are well above the frequencies of interest. The effective transfer function of the acceleration switching valve first-stage hydraulic amplifier is:

$$\frac{X(s)}{M(s)} = \frac{9.56 \times 10^{-2}}{s + 2.6}\ \frac{in/sec}{UNB}. \qquad (52)$$

Second-Stage Hydraulic Amplifier

Electrical Analogy. Referring once again to Figure 1 (Chapter I, Page 3), it may be seen that with zero lap on the valve spool (as is the case with the acceleration switching valve), the second-stage hydraulic amplifier is a simple series circuit as the valve spool moves from its null position. This condition is illustrated in Figure 1(a). As the spool moves either to the right or left it closes the orifice to one of the load and exhaust lines thereby eliminating the parallel path. Consider the case when the spool moves to the right. This action uncovers Supply Orifice A and Return Orifice B, and it covers Supply Orifice B and Return Orifice A. In this case the electrical analog is the simple series circuit shown in Figure 12. When the spool moves to the left, the electrical analog will be the reverse of this, but due to the fact that it has matched orifices, the same numerical values are still valid. This result is assuming that the leakage flow is negligible.

Characteristics Curves.

Derivation. The $P_L - Q_L$ curves for the second-stage hydraulic amplifier may be found by solving the circuit equations for Figure 12; therefore, we have:

$$P_s - P_{SA} - P_L - P_{RB} = 0, \text{ and} \tag{53}$$

$$Q_{SA} = Q_L = Q_{RB}. \tag{54}$$

Combining Equations 53 and 54 with the orifice equation yields:

$$P_L = P_s - \frac{Q_L^2}{g_{SA}^2} - \frac{Q_L^2}{g_{RB}^2}. \tag{55}$$

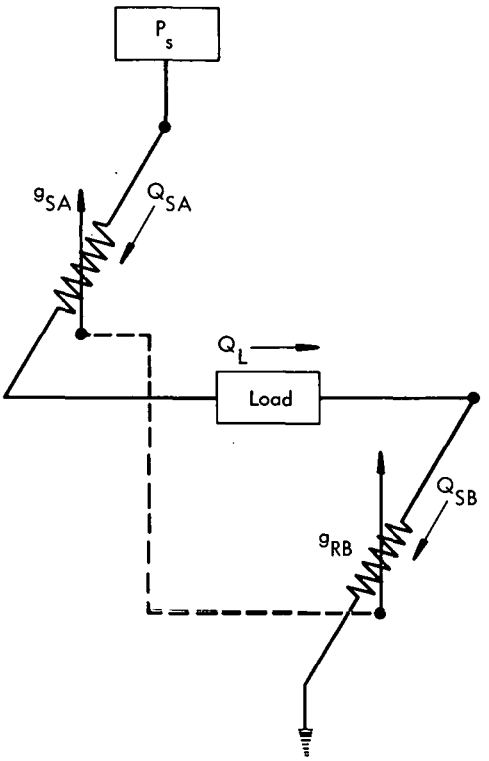

FIGURE 12

ELECTRICAL ANALOG OF THE SECOND-STAGE HYDRAULIC AMPLIFIER

Since the orifices are matched, Equation 55 becomes:

$$P_L = P_s - \frac{2 Q_L^2}{g^2}, \text{ or} \tag{56}$$

$$P_L = P_s - \frac{2}{x^2} \frac{\rho Q_L^2}{8 \pi^2 r_m^2 C_D^2}. \tag{57}$$

The $P_L - Q_L$ curves may be plotted from Equation 57. Figure 13 shows the $P_L - Q_L$ curves in the region near the origin considering small input perturbations.

Differential Coefficients and Transfer Function. From the curves in Figure 13 the differential coefficients may be obtained. The flow sensitivity is given by:

$$C_L = \left. \frac{\partial Q_L}{\partial x} \right|_{P_L = \text{CONST}} = \lim_{\Delta x \to 0} \left. \frac{\Delta Q_L}{\Delta x} \right|_{P_L = \text{CONST}}, \tag{58}$$

$$\simeq \left. \frac{\Delta Q_L}{\Delta x} \right|_{P_L = \text{CONST}} = \frac{0.47 - 0.00}{0.0005 - 0.0000}, \text{ or}$$

$$\simeq 940 \frac{\text{in}^3/\text{sec}}{\text{in}}.$$

The stiffness coefficient is given by:

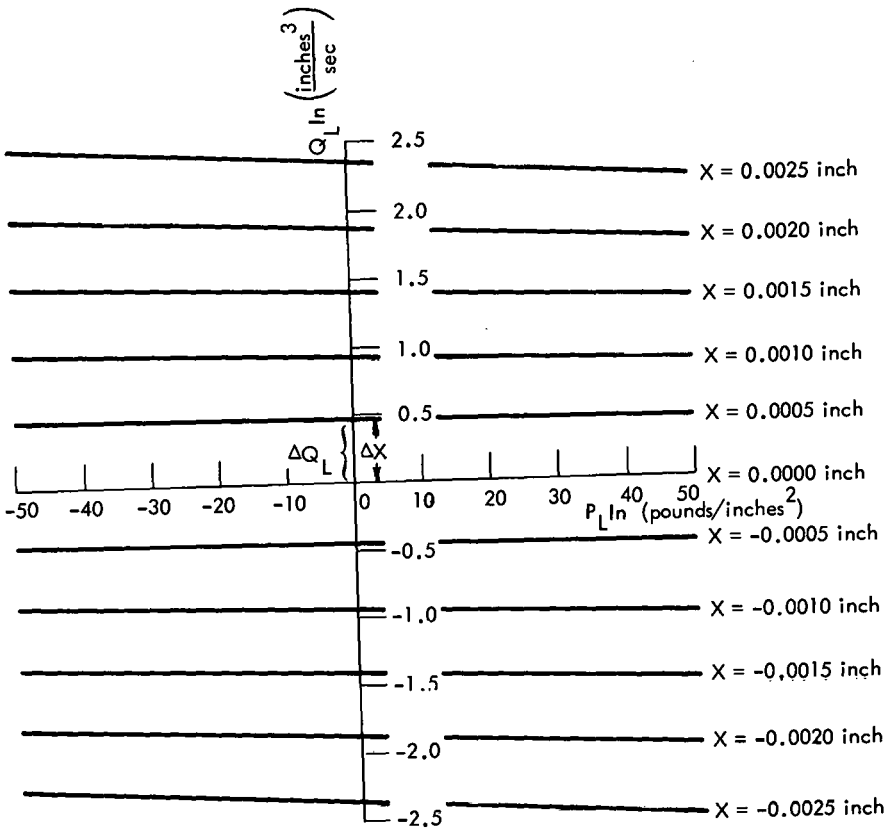

FIGURE 13

CHARACTERISTIC $P_L - Q_L$ CURVE OF SECOND-STAGE HYDRAULIC AMPLIFIER FOR CONSTANT VALUES OF SPOOL DISPLACEMENT

$$K_L = \frac{\partial Q_L}{\partial P_L}\bigg|_{x=\text{CONST}} = \lim_{\Delta P_L \to 0} \frac{\Delta Q_L}{\Delta P_L}\bigg|_{x=\text{CONST}}, \tag{59}$$

$$\simeq \frac{\Delta Q_L}{\Delta P_L}\bigg|_{x=\text{CONST}} = \frac{0.00 - 0.00}{10.0 - 0.0}, \text{ or}$$

$$\simeq 0.00 \ \frac{\text{in}^3/\text{sec}}{\text{lb/in}^2}.$$

The schematic diagram of the output stage and load is shown in Figure 14. This configuration may be analyzed by the same technique utilized in analysis of the first-stage hydraulic amplifier.[8] The equation describing the motion of the actuator is:

$$A_L \frac{dy}{dt} = \left| K_L \right| x - \left| C_L \right| P_L - Q_{l_L} - 1/2 \left(\frac{V_{i_L}}{\beta} \right) \frac{dP_L}{dt}. \tag{60}$$

Now the load pressure, P_L, is equal to the forces that react against it. These forces are given by:

$$\Sigma F_L = M_L \frac{d^2y}{dt^2} + f_L \frac{dy}{dt} + F_L, \tag{61}$$

where F_L represents the external forces acting upon the load. These forces are generally random in nature, and it is assumed that the effect of these random forces may be neglected. We have also assumed that due to the large diameter of the connecting lines and the relatively large mass of the load, the inertial and viscous effects of the fluid are negligible. Therefore, substituting the numerical values

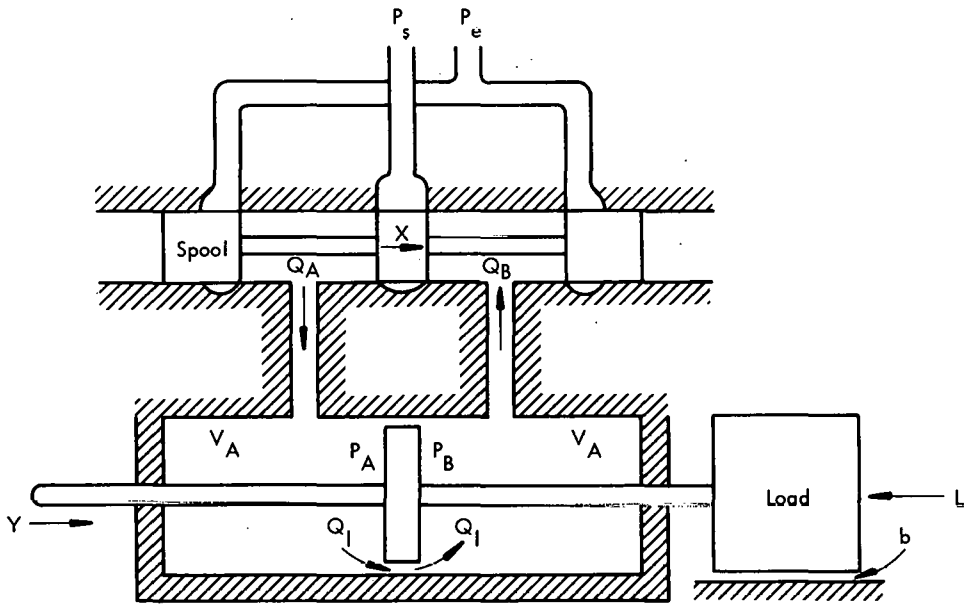

FIGURE 14

SCHEMATIC DIAGRAM OF THE SECOND-STAGE HYDRAULIC AMPLIFIER AND LOAD

into Equation 61 yields:

$$\Sigma F_L = 0.141 \frac{d^2y}{dt^2} + 0.233 \frac{dy}{dt}, \tag{62}$$

and Equation 60 then becomes:

$$A_L \frac{dy}{dt} = \left| C_L \right| \times - \left| K_L \right| \frac{\Sigma F_L}{A_L} - Q_{i_L} - 1/2 \left(\frac{V_{i_L}}{\beta} \right) \frac{d}{dt} \left(\frac{\Sigma F_L}{A_L} \right). \tag{63}$$

Substituting the numerical values in Equation 63 results in:

$$5.86 \frac{dy}{dt} = 940 \frac{in^3/sec}{in} - 9.06 \times 10^{-3} \frac{in^5}{lb\text{-}sec} \left(0.141 \frac{d^2y}{dt^2} + 0.233 \frac{dy}{dt} \right) \frac{1}{5.86\ in^2} -$$

$$1/2 \left(\frac{16.5\ in^2}{2.5 \times 10^5\ lb/in^2} \right) \frac{d}{dt} \left(0.141 \frac{d^2y}{dt^2} + 0.233 \frac{dy}{dt} \right) \frac{1}{5.86\ in^2}. \tag{64}$$

As may be seen, the effects of leakage and compressability are negligible; therefore, Equation 64 becomes:

$$5.86\ in^2 \frac{dy}{dt} = 940 \frac{in^3/sec}{in} \times - 1.55 \times 10^{-3} \frac{in^3}{lb\text{-}sec} \left(0.141 \frac{d^2y}{dt^2} + \right.$$

$$\left. 0.233 \frac{dy}{dt} \right) - 5.63 \times 10^{-6} \left(0.141 \frac{d^3y}{dt^3} + 0.233 \frac{d^2y}{dt^2} \right). \tag{65}$$

Collecting terms we have:

$$0.794 \times 10^{-6} \frac{d^3y}{dt^3} + (1.55 \times 10^{-6} + 0.218 \times 10^{-3}) \frac{d^2y}{dt^2} +$$

$$(5.86 + 0.361 \times 10^{-3}) \frac{dy}{dt} = 940 \frac{in^3/sec}{in} x. \quad (66)$$

Assuming quiescent initial conditions and taking the Laplace transform of Equation 66 we have:

$$(1.35 \times 10^{-7} s^2 + 3.76 \times 10^{-5} s + 1) 5.86 s Y(s) = 940 \frac{in^3/sec}{in} X(s). \quad (67)$$

The roots of the quadratic are at $s = (-1.40 \pm j 90) 10^2$ which are well above the frequencies of interest. Equation 67, therefore, becomes approximately:

$$Y(s) = \frac{160/sec}{s} X(s). \quad (68)$$

Combined Transfer Function

When Equation 52 is combined with Equation 68, we have the transfer function of the acceleration switching valve and hydrostatic slide combination. The transfer function, therefore, is:

$$\frac{Y(s)}{M(s)} = s \frac{15.3}{(s + 2.6)} \frac{in/sec^2}{UNB} . \quad (69)$$

Experimental Results

The theoretical derivation was checked by a frequency response test. The circuit configuration is shown in Figure 15(a). The relation for the transfer function is:

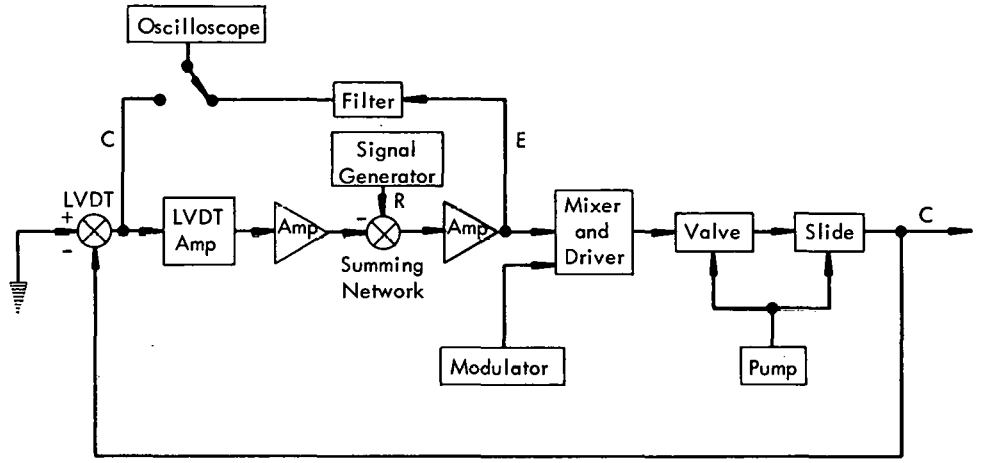

(a) Block diagram of the system configuration for frequency response test

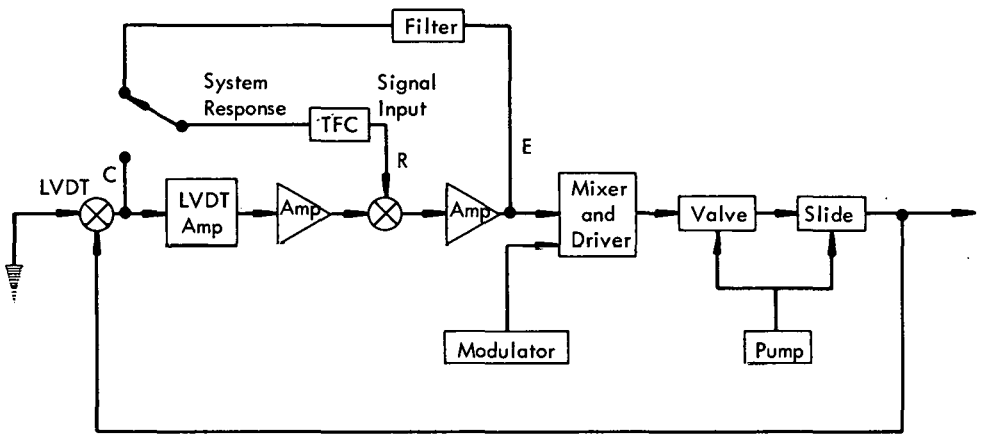

(b) Block diagram of the system configuration for system test utilizing the transfer function computer

FIGURE 15

SYSTEM CONFIGURATIONS FOR MEASURING THE ACCELERATION SWITCHING VALVE SYSTEM TRANSFER FUNCTION

$$KG(s) = \frac{C(s)}{E(s)}. \tag{70}$$

The output, C(s), and input, E(s), were measured separately, as shown in Appendix A (Page 95). A tabulation of the data obtained from this test is shown in Table I, and the plot of the frequency response of the acceleration switching valve and actuator combination is shown in Figure 16. Because of the system noise in the output of the final amplifier, the filter is necessary for accurate measurement.

As may be seen from Figure 16, the response falls off at the rate of 6 db/octave in the lower frequency range and at the rate of 12 db/octave in the higher frequency range. The break frequency is at approximately 0.54 cycle per second. The indicated transfer function is:

$$KG(s) = \frac{2\pi(0.58)(2\pi)(0.54)}{s(s + 2\pi(0.54))} \frac{in/sec^2}{UNB}, \text{ or} \tag{71}$$

$$= \frac{12.3}{s(s + 3.39)} \frac{in/sec^2}{UNB}.$$

The transfer function of the acceleration switching valve and actuator combination was also measured by the transfer function computer. This instrument is basically one which compares the output signal with the input and its differentials. The transfer function is then obtained from the amount of differential signals that it takes to balance the input with the output.

The transfer function that was obtained by this method was:

$$KG(s) = \frac{13.8}{s(s + 3.5)} \frac{in/sec^2}{UNB}. \tag{72}$$

TABLE I

DATA FROM FREQUENCY RESPONSE TEST

Frequency (In Cycles Per Second)	C (jw) (In Volts)	E (jw) (In Volts)	$\frac{C(jw)}{E(jw)}$ (In Volts/Volt)	$\frac{C(jw)}{E(jw)}$ (In $\frac{In/Sec}{\% UNB}$)	$\frac{C(jw)}{E(jw)}$ (In DB)	Filter Response (In DB)	KG(s) (In DB)
0.01	0.0005	0.055	110	55	34.8	0.00	34.8
0.02	0.001	0.055	55	27.5	28.8	0.00	28.8
0.04	0.002	0.055	27.5	13.7	22.8	0.00	22.8
0.06	0.004	0.055	13.7	6.85	16.8	0.00	16.8
0.08	0.005	0.055	11.0	5.5	14.8	0.00	14.8
0.1	0.006	0.055	9.12	4.56	13.2	0.00	13.2
0.15	0.008	0.055	6.87	3.44	10.8	0.00	10.8
0.2	0.010	0.055	5.5	2.75	8.8	0.00	8.8
0.3	0.020	0.055	2.75	1.37	2.8	0.00	2.8
0.4	0.030	0.055	1.83	0.915	- 0.7	0.00	- 0.7
0.5	0.040	0.055	1.37	0.685	- 3.2	0.00	- 3.2
0.6	0.054	0.056	1.02	0.51	- 5.8	0.00	- 5.8
0.8	0.076	0.060	0.79	0.395	- 8.0	0.00	- 8.0
1.0	0.116	0.062	0.535	0.267	-11.4	0.00	-11.4
1.5	0.230	0.066	0.287	0.143	-16.8	0.00	-16.8
2.0	0.340	0.068	0.189	0.0945	-20.5	0.00	-20.5
3.0	0.650	0.080	0.122	0.061	-24.3	- 4.1	-28.4
4.0	0.580	0.078	0.134	0.067	-23.5	-10.1	-33.6
5.0	0.330	0.070	0.212	0.106	-19.5	-18.1	-37.6
6.0	0.160	0.058	0.363	0.182	-14.8	-24.1	-38.9
8.0	0.064	0.040	0.625	0.312	-10.1	-33.2	-43.3
10.0	0.032	0.032	1.00	0.500	- 6.0	-41.2	-47.2
12.0	0.017	0.027	1.59	0.795	- 2.0	-48.8	-50.8
14.0	0.008	0.025	3.12	1.56	- 3.9	-56.1	-52.2
16.0	0.006	0.016	2.67	1.33	2.5	-58.0	-55.5
18.0	0.004	0.014	3.5	1.75	4.9	-64.1	-59.2
20.0	0.003	0.014	4.66	2.33	7.4	-70.1	-62.7

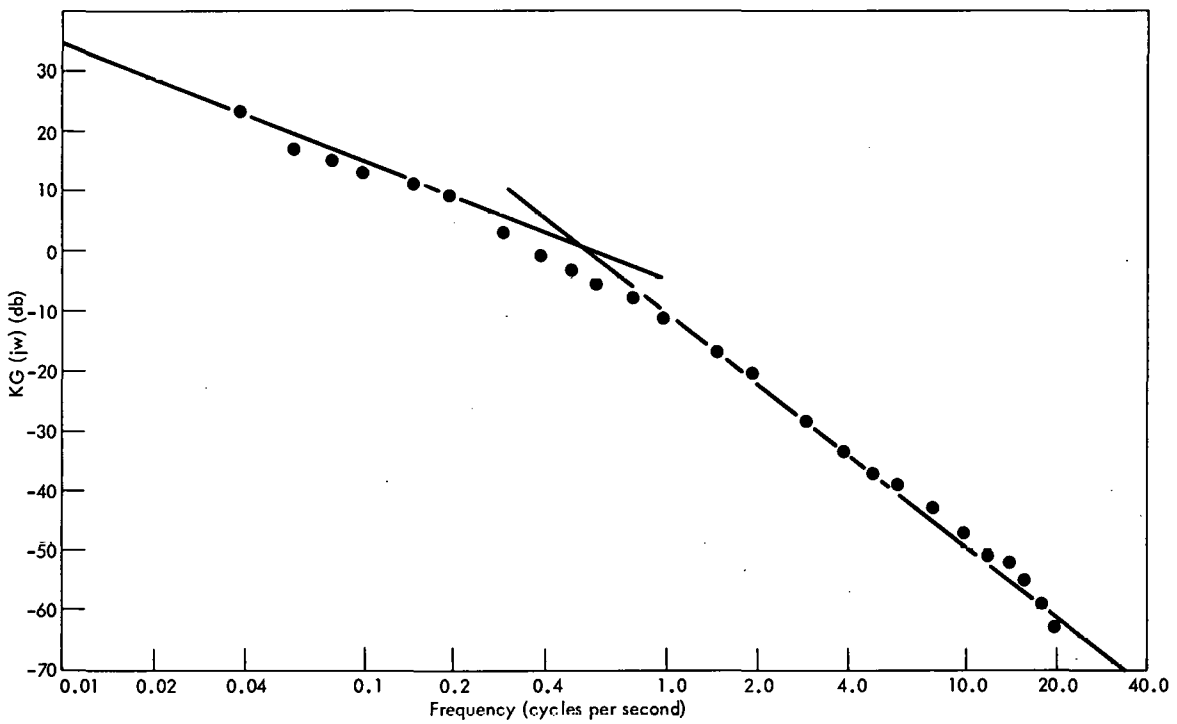

FIGURE 16

FREQUENCY RESPONSE OF ACCELERATION SWITCHING VALVE SYSTEM

This relationship compares well, within the precision of the measurement technique, with that obtained by the frequency response technique.

Equations 71 and 72 compare reasonably well with Equation 69 considering that: (1) linearity is assumed, (2) noise is a problem in measurement, (3) the system characteristics vary with ambient conditions, (4) perfect machining is assumed within the acceleration switching valve, and (5) the hydraulic fluid and valve is assumed to be free from contamination.

In the design of the system, Equation 69 will be assumed to be valid. In spite of the fact that there is closer agreement between Equations 71 and 72, Equation 69 was chosen for design purposes primarily because it will tend to give more pessimistic results.

CHAPTER IV

MACHINE TOOL CONTROL SYSTEMS

Design Criteria

Since design specifications generally depend upon the system application and are often determined by an intuitive process, let us discuss machine tool control systems in general. Small rise and settling times are certainly desirable characteristics in order that errors may be reduced rapidly, and overshoot should be minimized in order to prevent excessive metal removal. The final speed, accuracy, and usefulness of the automatic machine tool is determined by the combined characteristics of the control system and the machine tool.[17] Often in the case of machine tools, noise, vibration, mechanical deflection, and resistance to load disturbances are the determining factors in the usefulness of control systems.

An automatic lathe is a contouring device. The normal input is seldom uniquely a step, ramp, or parabolic function; but it is, in general, a combination of these. The function of the control system is to maintain the trajectory and velocity of the cutting tool with essentially zero error with respect to the command input. The position, velocity, and acceleration errors, therefore, are also very important. The relative importance that should be assigned to each of these is open to conjecture, and this will be, in part, discussed in the sections that follow.

Optimization

Specifications are generally in terms of frequency response or intuitive concepts of rise time and overshoot. These are generally minimum requirements of the system, and they give no information about the optimum location of poles and zeros. If, however, there was a criterion which would specify the exact form of the optimum transient response, this would be equivalent to specification of the desired system transfer function.[18] Such criteria have been developed, and they are commonly known as indices of performance (or cost function in modern control theory). Their application to system synthesis is known as optimization. Optimization does not specify the degree of stability, but it is rather a part of the solution. An advantage of this approach is its ability to detect an inconsistent set of specifications.[19]

In general, an index of performance should have the following properties: (1) reliability, (2) ease of application, and (3) selectivity.[19,20] There is no question but that an index of performance should be reliable. The more commonly used indices of performance may be mechanized on an analog computer (see Appendix C, Page 106),[21] and a digital computer is almost unlimited in this respect. Optimization does not require analyticity if a computer is available; however, one tends to lose an insight into the system if complete dependence is placed on a computer. On the other hand, great selectivity tends to create a false impression of the value of the system if its parameters are somewhat removed from the optimum. Selection of an index of performance, therefore, should not depend entirely upon selectivity or analyticity.

Two of the more common indices of performance are:

$$I_1 = \int_o^\infty t \left| e(t) \right| dt, \text{ and} \tag{73}$$

$$I_2 = \int_o^\infty [e(t)]^2 dt. \tag{74}$$

I_1 is known as the ITAE criterion which is the most selective of the commonly used indices of performance. I_2 is the rms error (RMSE) criterion which is the most popular index of performance because of its amenability of mathematical manipulation.[19]

Intuitive reasoning would seem to indicate that an importance weighting-versus-error curve should have the shape shown in Figure 17 where "A" is the tolerance limits.[22] This, however, does not take into account the fact that, in the case of machine tools, set up and operating inaccuracies form a major portion of the error in the final product. The control system, therefore, should maintain the system error as small as possible with no error considered negligible. There are also such practical considerations as tool wear and machine inaccuracies which indicate that the control system should maintain the system error as small as possible.

The RMSE criterion places emphasis on the error according to the square of its magnitude. Large errors, therefore, are emphasized more than small errors. This condition results in comparatively large overshoots.[22] The ITAE criterion, however, emphasizes error magnitude equally, and it also penalizes an error for the length of time it lingers, a situation that results in a relatively small overshoot.

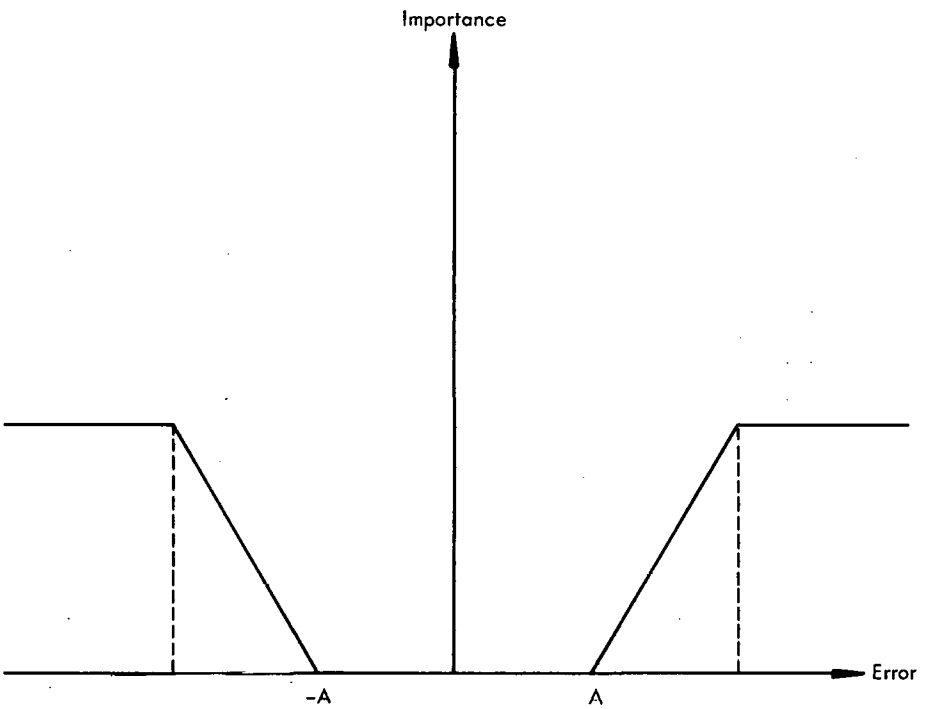

FIGURE 17

ERROR-WEIGHTING FUNCTION BASED

ON INTUITIVE REASONING

Since the machine tool control system should maintain small errors with a minimum overshoot, the ITAE criterion would seem to be the superior index of performance for this application. There has been no rigorous justification for the selection of this criterion, however. Rather, it was based on intuitive reasoning. A case has been presented for the ITAE criterion, but this should not imply that a system satisfying the RMSE criterion is unacceptable.

It appears that a single index of performance cannot be selected as the ultimate for all types of control systems. The selection of such a criterion depends upon the system application and the facilities available. It may also depend upon the desired type of analysis, or it may be based upon some practical consideration not directly related to the system transient response. In the final analysis, the selection of an index of performance is largely a matter of judgment.

It should not be considered that optimization is a panacea for system design. It is a tool to be used along with other available tools in conjunction with engineering judgment to facilitate the logical synthesis of feedback control systems.

Approximate Optimization

The synthesis of the optimum system may be approximated by root-locus techniques by the following procedure:

1. Select an acceptable range of damping ratios and undamped natural frequencies from practical considerations.

2. From Step 1 construct a region of acceptability in the s-plane.

3. Shape the locus of the system to pass through the region of acceptability.

4. Determine the allowable velocity error from practical considerations.

5. Determine the compensation necessary to fulfill the requirements of Step 4.

6. Determine if the locus still passes through the region of acceptability. If the locus does not pass through the region of acceptability, repeat Steps 3 through 6.

This system should approximate the optimum system.

It should be emphasized that the transfer function of the system depends upon many factors such as the ambient temperature of the oil, and dissolved air and/or contamination in the oil. Furthermore, hydraulic control systems are inherently nonlinear. Therefore, a rigorously exact optimization procedure based on linear, time-invariant techniques is inherently approximate.

The use of step functions as the test input when this is not the normal command input is not immediately obvious. Graham and Lathrop have stated, however, "Systems with good response to step functions of input displacement, and small but finite velocity and acceleration errors, probably represent an overall optimum."[18] Now machine tool control systems must closely approximate a zero velocity error system since it is primarily a contouring device. Type 2 systems, however, will usually have large overshoots; therefore, a small but finite velocity error is a desirable characteristic. The statement of Graham and Lathrop should be generally applicable to machine-tool systems.

Specifications

Two possible methods of specification and their normal ranges for machine tools are the following: (1) bandwidth - 20 to 120 radians/sec, and (2) velocity error - 0.0002 to 0.001 in/in/min.[17] These, in conjunction with some restriction on overshoot, approximately specify the acceptable transient response of the control system.

For Type 1 systems the ITAE criterion yields an optimum damping ratio of $\zeta = 0.7$.[18,20] For Type 2 systems, however, the system improves continually with increasing damping ratio. There is negligible improvement above a damping ratio of $\zeta = 1.0$, and there is very little improvement above a damping ratio of $\zeta = 0.9$.[18] For Type 1 systems the RMSE criterion is $\zeta = 0.5$.[20] The optimum system, therefore, may be approximated by a system with a damping ratio of between $\zeta = 0.5$ and $\zeta = 0.9$.

Although consideration is given only to deterministic inputs, actual control-system performance depends on many factors among which are system stiffness, response to residual noise, and sensitivity. It should be noted that a large system bandwidth also presents a large pass band to noise. Therefore, an approximate method of limiting noise effects is to restrict the system bandwidth. Let us, therefore, choose a maximum system bandwidth of 75 radians per second (approximately 12 cycles per second) to limit noise effects. Also, to insure sufficient transient response, let us choose a minimum bandwidth of 50 radians per second (approximately 8 cycles per second). The actual system bandwidth should fall

somewhere between these extremes, and we shall choose 62.8 radians per second (10 cycles per second) as the design center.

The previously suggested range of velocity errors is from 0.0002 to 0.001 in/in/min. In the case of high-precision machining applications, however, this would seem to be too great for most reasonable cutting speeds. The system velocity error, therefore, is chosen to be no greater than 0.00002 in/in/min.

There are now sufficient specifications to design the system. These specifications are the following:

Bandwidth - $50 \leq \omega_n \leq 75$ radians/sec,

Damping Ratio - $0.5 \leq \zeta \leq 0.9$,

Velocity Error - $E_v \leq 0.00002$ in/in/min.

The s-plane plot indicating the region of acceptability is shown in Figure 18. In this figure are plotted damping ratios of $\zeta = 0.5$, 0.9, and 0.7. These are the minimum, maximum, and design-center damping ratios, respectively. Also plotted are undamped natural frequencies of $\omega_n = 50$, 75, and 62.8 radians per second. These are the minimum, maximum, and design-center undamped natural frequencies, respectively. The intersection of the $\zeta = 0.7$ and $\omega_n = 62.8$ radians per second lines is the point through which it is desired that the locus of the system pass. A system operating point anywhere within the shaded area indicated on Figure 18, however, should be considered as acceptable.

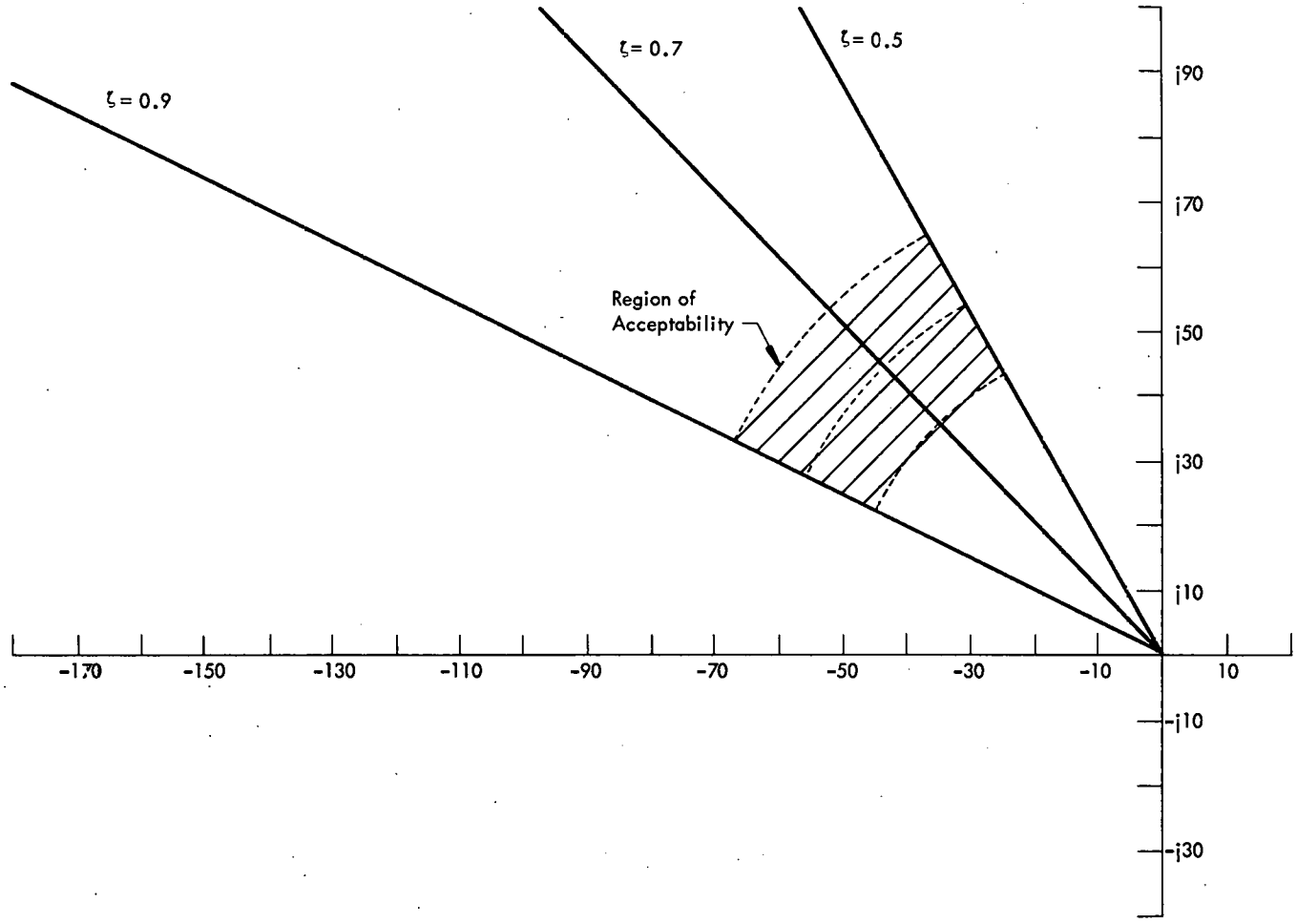

FIGURE 18

REGION OF ACCEPTABILITY FOR THE ACCELERATION SWITCHING VALVE AND HYDROSTATIC SLIDE CONTROL SYSTEM

CHAPTER V

SYSTEM DESIGN

The Uncompensated System

The transfer function of the uncompensated acceleration switching valve and hydrostatic slide system as developed in Chapter III (Page 23) is:

$$\frac{Y(s)}{M(s)} = \frac{15.3}{s(s+2.6)} \text{ in/sec}^2/\text{UNB.} \tag{75}$$

The uncompensated system is essentially a second-order system with poles at $s = 0$ and $s = -2.6$. Although there are higher-order poles, these are well above the control frequencies. The root locus of the uncompensated system is shown in Figure 19. As may be seen, the locus of the uncompensated system is far removed from the region of acceptability. The uncompensated system is also very lightly damped for any reasonable value of gain. It is now desired to find the proper system compensation so that the system will fulfill the design specifications.

Compensation

Before designing the proper system compensation it would be desirable to discuss compensation in general. The purpose of compensation, in this case, is to improve the transient response of the system. The locus must be moved further to the left away from the imaginary axis. It is also possible that the steady-state velocity error of the system may need improvement.

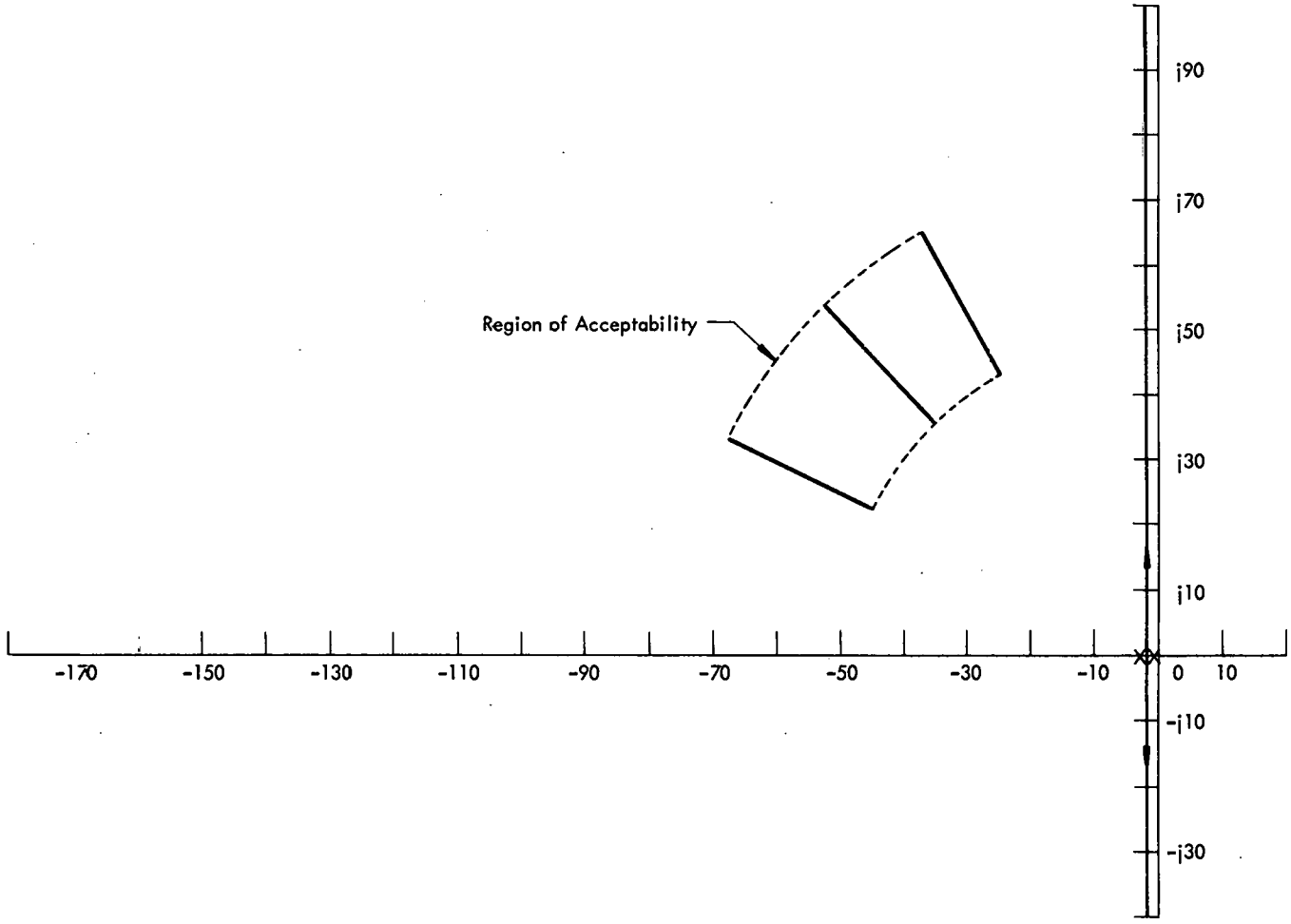

FIGURE 19

ROOT LOCUS OF THE UNCOMPENSATED ACCELERATION SWITCHING VALVE AND HYDROSTATIC SLIDE CONTROL SYSTEM

To accomplish this task, either series or parallel compensation may be used. There are advantages and disadvantages to both which must be considered before choosing between the two. Some of these are the following:

1. Feedback compensation may not be as readily applied.

2. Depending upon the physical form of the system, a practical series or parallel compensation may not exist.

3. Economic considerations may be the determining factor; i.e., series compensation may require more amplifiers and larger components.

4. Noise may be the determining factor; i.e., series compensation may require greater amplication thereby accentuating the noise problem.

5. Often faster time response may be obtained with parallel compensation.[20]

Parallel Compensation. The ultimate choice between series and parallel compensation more often than not results from practical considerations rather than an inherent difference in transient response.[20] In the acceleration switching valve system there is not a convenient feedback path to apply compensation by passive networks, so parallel compensation is limited to such external transducers that will operate on the physical characteristics of the system.

There is available both velocity and acceleration transducers; therefore, let us first examine acceleration transducers. Referring to the block diagram in Figure 20, the transfer function of the minor loop is given by:

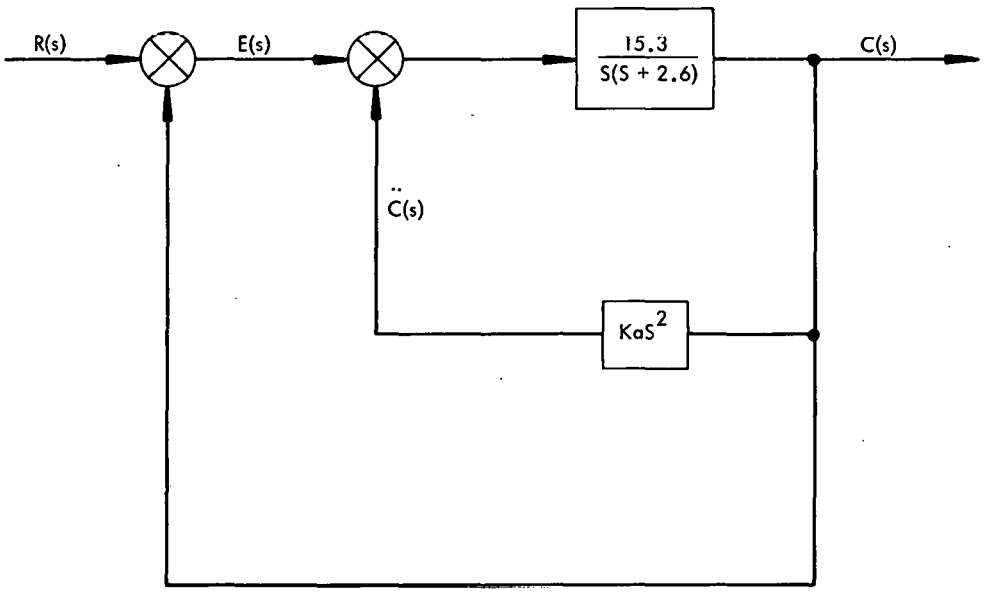

FIGURE 20

BLOCK DIAGRAM OF THE ACCELERATION SWITCHING VALVE CONTROL SYSTEM UTILIZING ACCELERATION FEEDBACK

$$\frac{C(s)}{E(s)} = \frac{\frac{15.3}{s(s+2.6)}}{1 + K_a s^2 \frac{15.3}{s(s+2.6)}}, \text{ or} \tag{76}$$

$$= \frac{15.3}{s(s+2.6) + (K_a s^2)(15.3)}, \text{ or}$$

$$= \frac{15.3}{s\left[(1+K_t)s + 2.6\right]}, \text{ or}$$

$$= \frac{\frac{15.3}{1+K_t}}{s\left(s + \frac{2.6}{1+K_t}\right)}.$$

Examination of Equation 76 indicates that the use of an acceleration transducer moves the pole of the system further to the right on the imaginary axis. Since this is not the direction in which it is desired to move the pole, acceleration transducers will be eliminated from further consideration.

Returning to velocity transducers there is available a linear velocity transducer. This component consists of a coil wound in a nonmagnetic case. A magnetic core, which is free to move inside the case, induces a voltage in the coil proportional to the rate at which the core is moving. By connecting the case to the stationary member and the magnetic core to the moving member, a signal may be obtained which is proportional to the relative velocity between the stationary and moving members.

The transfer function of the velocity transducer is:

$$\frac{K_v s}{\tau_v s + 1}, \tag{77}$$

but since the time constant, τ_v, is very small, the transfer function is effectively:

$$K_v s. \tag{78}$$

When the velocity transducer is added to the system, the block diagram takes the form of Figure 21. The transfer function of the minor loop is:

$$\frac{C(s)}{E(s)} = \frac{K \frac{Z(s)}{P(s)}}{1 + K_v s \frac{K Z(s)}{P(s)}}. \tag{79}$$

The characteristic equation of the minor loop of the acceleration switching valve is, therefore,

$$s(s + 2.6) + 15.3 K_v s = s^2 + (2.6 + 15.3 K_v) s, \text{ or} \tag{80}$$

$$= s(s + K_m).$$

Velocity feedback, therefore, has the effect of moving the pole of the acceleration switching valve further to the left on the negative real axis. This action has the desired stabilizing effect on the system.

Referring to Equation 79, we have the equation for the open-loop transfer function of the acceleration switching valve utilizing velocity feedback. Substituting Equation 75 into Equation 79 we have:

$$\frac{C(s)}{E(s)} = \frac{15.3}{s(s + 2.6 + 15.3 K_v)}. \tag{81}$$

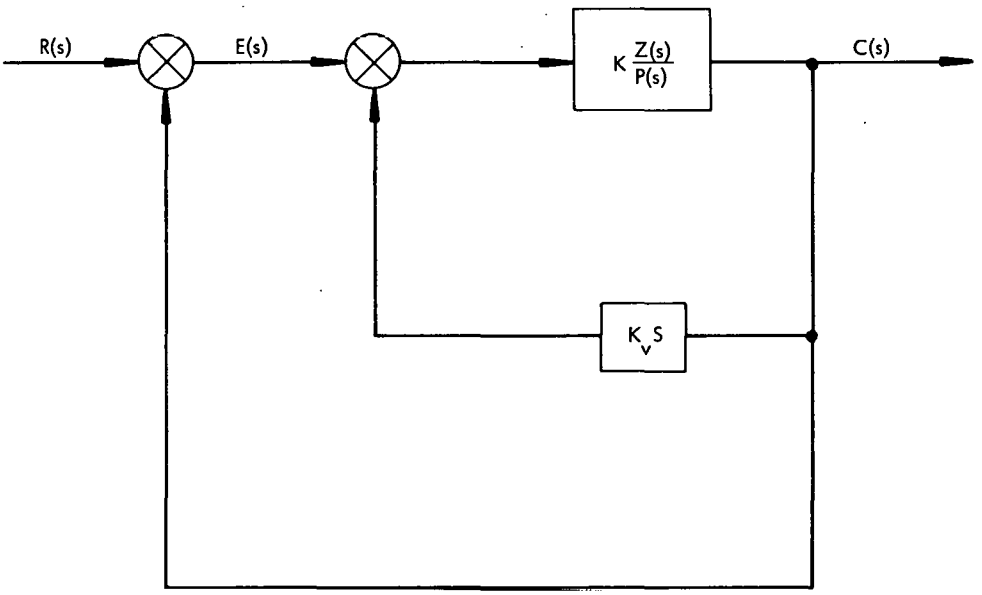

FIGURE 21

BLOCK DIAGRAM OF ACCELERATION SWITCHING VALVE

SYSTEM UTILIZING A VELOCITY TRANSDUCER

Referring to Figure 18 it is desired that the locus pass through the point $s = -44 \pm j\,44.5$. It is, therefore, desired that the open loop has poles at $s = 0, -88$. We have, therefore,

$$2.6 + 15.3\,K_v = 88, \text{ or} \tag{82}$$

$$K_v = 5.58.$$

The open-loop system is now described by Equation 83:

$$\frac{C(s)}{E(s)} = \frac{\dfrac{15.3}{s(s+2.6)}}{1 + 5.58\,s\,\dfrac{15.3}{s(s+2.6)}}, \text{ or} \tag{83}$$

$$= \frac{15.3}{s^2 + 2.6\,s + 85.4\,s}, \text{ or}$$

$$= \frac{15.3}{s(s+88)}.$$

The transfer function of the system is then given by:

$$\frac{C(s)}{R(s)} = \frac{\dfrac{15.3\,A}{s(s+88)}}{1 + \dfrac{15.3\,A}{s(s+88)}}, \text{ or} \tag{84}$$

$$= \frac{15.3\,A}{s^2 + 88\,s + 15.3\,A}.$$

The root locus of this system is shown in Figure 22. As may be seen, the root locus passes through the region of acceptability.

Let us now examine the velocity error. The velocity error is given by:

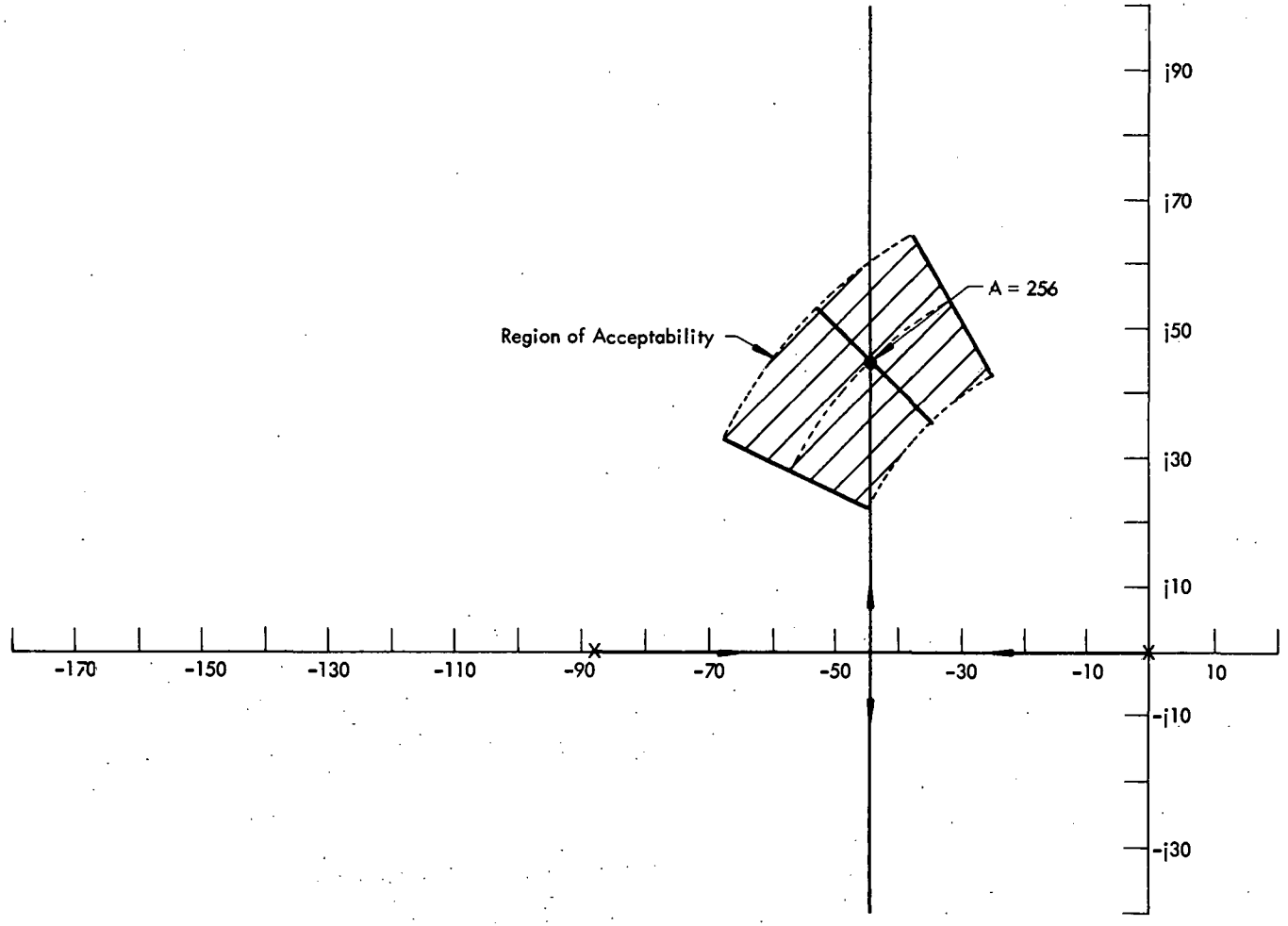

FIGURE 22

ROOT LOCUS OF ACCELERATION SWITCHING VALVE CONTROL

SYSTEM UTILIZING VELOCITY FEEDBACK

$$E_v = \frac{1}{K_v} = \frac{1}{\lim_{s \to 0} s \frac{(15.3)(256)}{s\,(s + 88)}}, \text{ or} \tag{85}$$

$$= \frac{88}{(15.3)(256)}, \text{ or}$$

$$= 0.0225 \text{ in/in/sec.}$$

In terms of minutes:

$$= \frac{0.0225}{60}, \text{ or}$$

$$= 0.000375 \text{ in/in/min.}$$

The velocity error is excessive and needs to be reduced by approximately a factor of 20; therefore, let us insert a lag network with a transfer function of:

$$KG_L(s) = \frac{K\,(s + 20)}{s + 1}. \tag{86}$$

The transfer function of the system then becomes:

$$\frac{C(s)}{R(s)} = \frac{15.3\,KA \frac{s + 20}{s\,(s + 88)(s + 1)}}{1 + 15.3\,AK \frac{s + 20}{s\,(s + 88)(s + 1)}}, \text{ or} \tag{87}$$

$$= \frac{15.3\,KA\,(s + 20)}{s^3 + 89\,s^2 + (88 + 15.3\,KA)\,s + 306\,KA}.$$

The root locus of this system is shown in Figure 23. The locus of this system passes through the region of acceptability, but it just barely passes through it. Although this is acceptable, it is desired that the locus pass more nearly through the design center. The locus may be moved to the left by increasing the gain of the velocity feedback path.

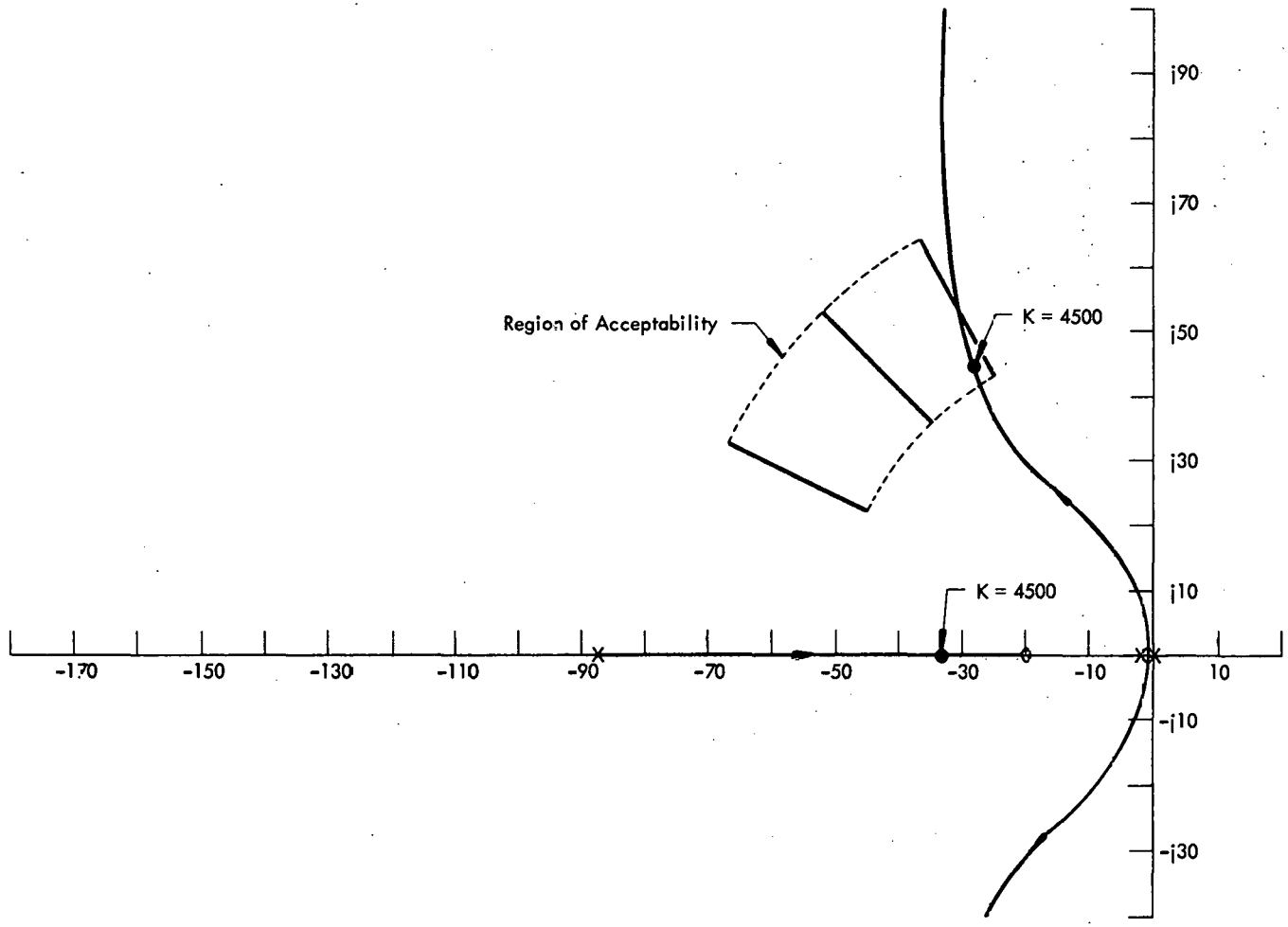

FIGURE 23

ROOT LOCUS OF SYSTEM UTILIZING VELOCITY FEEDBACK

AND LAG COMPENSATION

Now it is desired to have the locus approach infinity asymptotically to a line intersecting the negative real axis at s = -49. This intersection is given by:

$$\text{Intersection} = \frac{\Sigma \text{ Poles} - \Sigma \text{ Zeros}}{\text{Number of Poles} - \text{Number of Zeros}}, \text{ or} \tag{88}$$

$$= \frac{x - 1 - 0 + 20}{3 - 1} = -49.$$

Therefore,

$$x = -98 - 19, \text{ or}$$

$$= -117,$$

where "x" is the desired pole location. The transfer function is then given by:

$$\frac{C(s)}{R(s)} = \frac{K \dfrac{s + 20}{s(s + 117)(s + 1)}}{1 + \dfrac{K(s + 20)}{s(s + 117)(s + 1)}}, \text{ or} \tag{89}$$

$$= \frac{K(s + 20)}{s^3 + 118 s^2 + (117 + K) s + 20K}.$$

The root locus of this system is shown in Figure 24. With a gain of K = 6600, this has a dominant complex root at s = -41.5 ± j 44.5 which is near the design center.

The velocity error is given by:

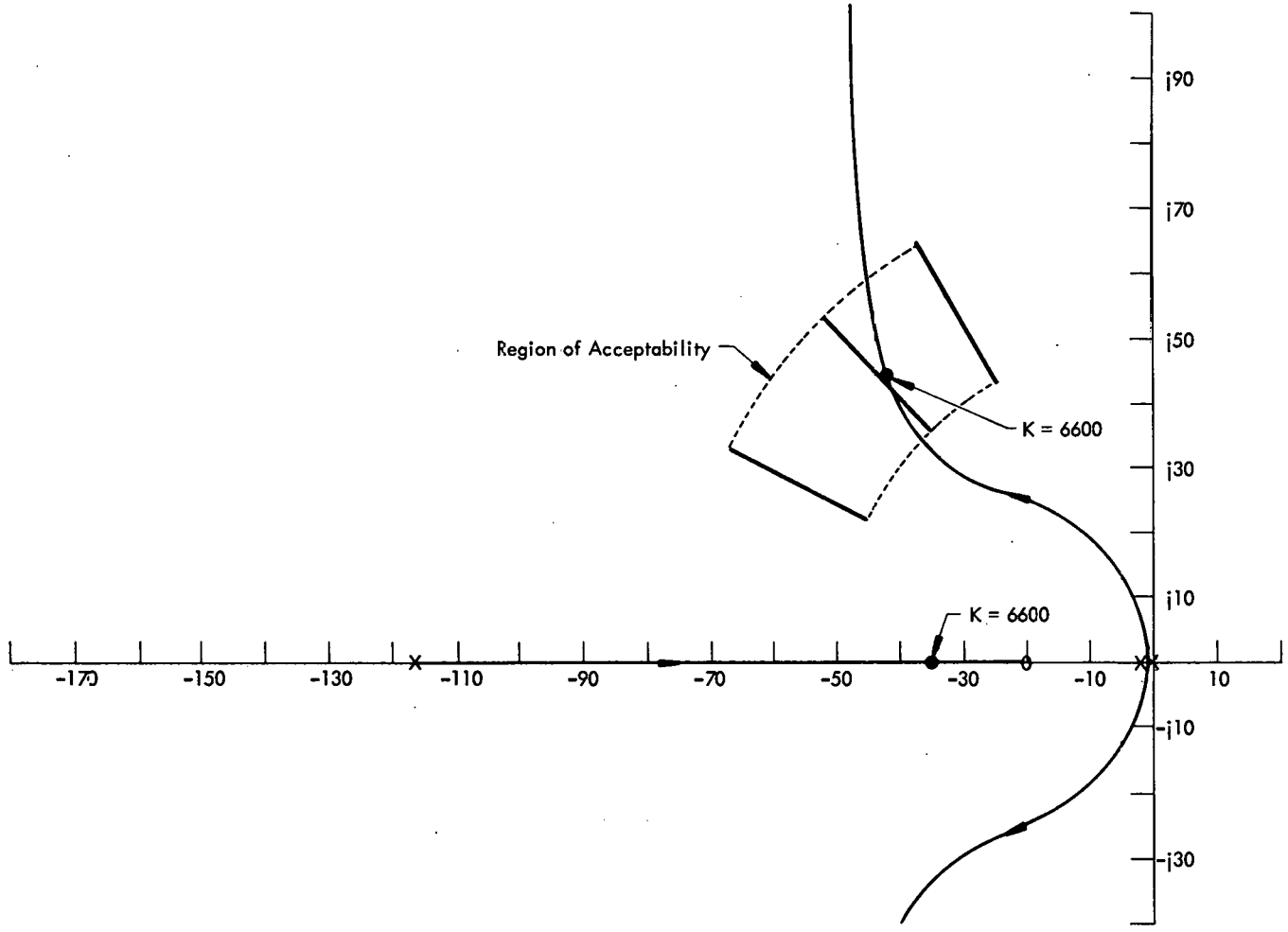

FIGURE 24

ROOT LOCUS OF FINAL SYSTEM UTILIZING VELOCITY FEEDBACK

$$E_v = \frac{1}{K_v} = \lim_{s \to 0} s \frac{1}{\frac{6600\,(s + 20)}{s\,(s + 117)(s + 1)}}, \text{ or} \qquad (90)$$

$$= \frac{117}{(6600)(20)}, \text{ or}$$

$$= 0.000885 \text{ in/in/sec.}$$

In terms of minutes:

$$= \frac{0.000885}{60}, \text{ or}$$

$$= 0.0000148 \text{ in/in/min.}$$

Figure 24 shows that we have a damping ratio of $\zeta = 0.69$ and an undamped natural frequency of $\omega_n = 61$ radians per second.

Using velocity feedback, a system has been designed which has the following characteristics:

$\omega_n = 61$ radians/second,

$\zeta = 0.69$, and

$E_v = 0.0000148$ inch/inch/minute.

This system is within the design specifications; however, let us consider the practical aspects of parallel feedback. It would seem from the theoretical point of view that parallel compensation is ideal in this application, but the previously described velocity transducer is difficult to mount due to its physical construction. It also tends to generate noise within the pass band of the system.

Of course, there is the possibility of using tachometer feedback. The physical mounting of a tachometer is even more inconvenient than is the previously

mentioned linear velocity transducer in this case. There is also friction and backlash in the gear train to consider. It appears, therefore, that if suitable transient response can be obtained by series compensation, it would not be desirable by virtue of practical considerations to use parallel compensation.

Series Compensation. Series compensation, in general, consists of integral, derivative, and/or cancellation compensation. Cancellation compensation is generally used to cancel undesirable complex poles. Since this system has no complex poles, cancellation compensation will be eliminated from further consideration. The general characteristics of integral and derivative compensation are the following:

1. Integral (or lag) compensation results in large increases in system gain and a small reduction in the undamped natural frequency.

2. Derivative (or lead) compensation results in small increases in system gain and a large increase in undamped natural frequency.[20,22]

In general, therefore, the lead network should be used to improve the transient response, and the lag network should be used to improve the velocity error.

It is now desired to shape the locus of the characteristic equation so that it has a dominant complex root which falls within the region of acceptability. Since it is desired to improve the transient response of the system, the use of a lead network is indicated. The location of this network in the s plane may be determined by utilizing the basic rules of root locus construction.

For a point to exist on the locus of the system, it must satisfy the equation:

$$\Sigma(\angle P) - \Sigma(\angle z) = (2K + 1)\ 180^{\circ},\ ^{20,22,23} \qquad (91)$$

where:

$\Sigma(\angle z)$ represents the sum of the angles from the point on locus to the zeros of the system,

$\Sigma(\angle P)$ the sum of the angles from the point on the locus to the poles of the system, and

k any integar 0, 1, 2, ---, n, ---.

The summation of angles from the poles and zeros of the original system to the desired root will result in some angle $180 + \emptyset$. It is necessary for the compensating network to contribute an angle $\emptyset_c = -\emptyset$, so that Equation 91 is once more satisfied.

A method for determining the desired lead network is set forth below.[20] The steps in this method are the following:

1. Locate the desired root, s_2, and draw lines through the origin to s_2 and horizontally to the left of s_2.

2. Draw the line bisecting the angle between these two lines.

3. Draw lines at an angle of $\emptyset\ c/2$ to either side of the bisector.

4. Using the intersection of the lines of Step 3 with the real axis, locate the desired pole and zero.

Considering the original system with poles at $s = 0$ and $s = -2.6$, it is desired to obtain roots to the characteristic equation at $s = -44 \pm j\ 44.5$. Referring

to Figure 25, note that the sum of the angles from the pole to the desired root is given by:

$$\theta = 134.5^\circ + 133^\circ = 267.5^\circ = 180^\circ + 87.5^\circ, \text{ or} \qquad (92)$$
$$= 180^\circ + \phi.$$

It is desired, therefore, that the compensating network provide an angular contribution of $\phi_c = -87.5^\circ$.

Performing the construction just indicated, we find that the desired lead network has a zero at $s = -27$ and a pole at $s = -149$. This is shown in Figure 25.

With this compensating network inserted in the forward path of the system, the transfer function of the system is given by:

$$\frac{C(s)}{R(s)} = \frac{\dfrac{K_t (s + 27)}{s(s + 2.6)(s + 149)}}{1 + \dfrac{K_t (s + 27)}{s(s + 2.6)(s + 149)}}, \text{ or} \qquad (93)$$

$$= \frac{K_t (s + 27)}{s^3 + 151.6\, s^2 + (387.4 + K_t)\, s + 27\, K_t}.$$

The root locus of this system is shown in Figure 26. The locus passes well within the region of acceptability. The velocity error is given by:

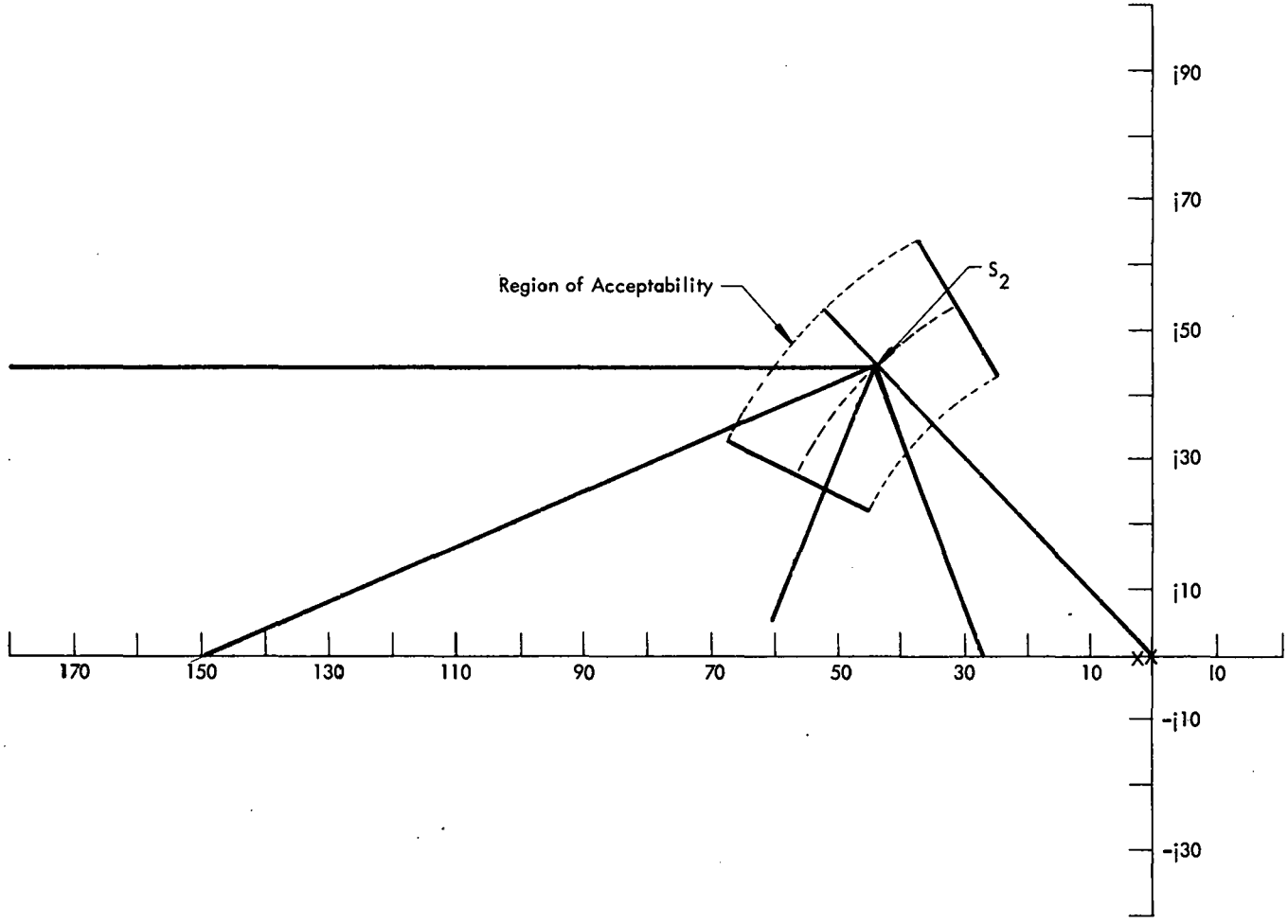

FIGURE 25

DETERMINATION OF DESIRED COMPENSATING NETWORK

SO THAT THE LOCUS PASSES THROUGH S_2

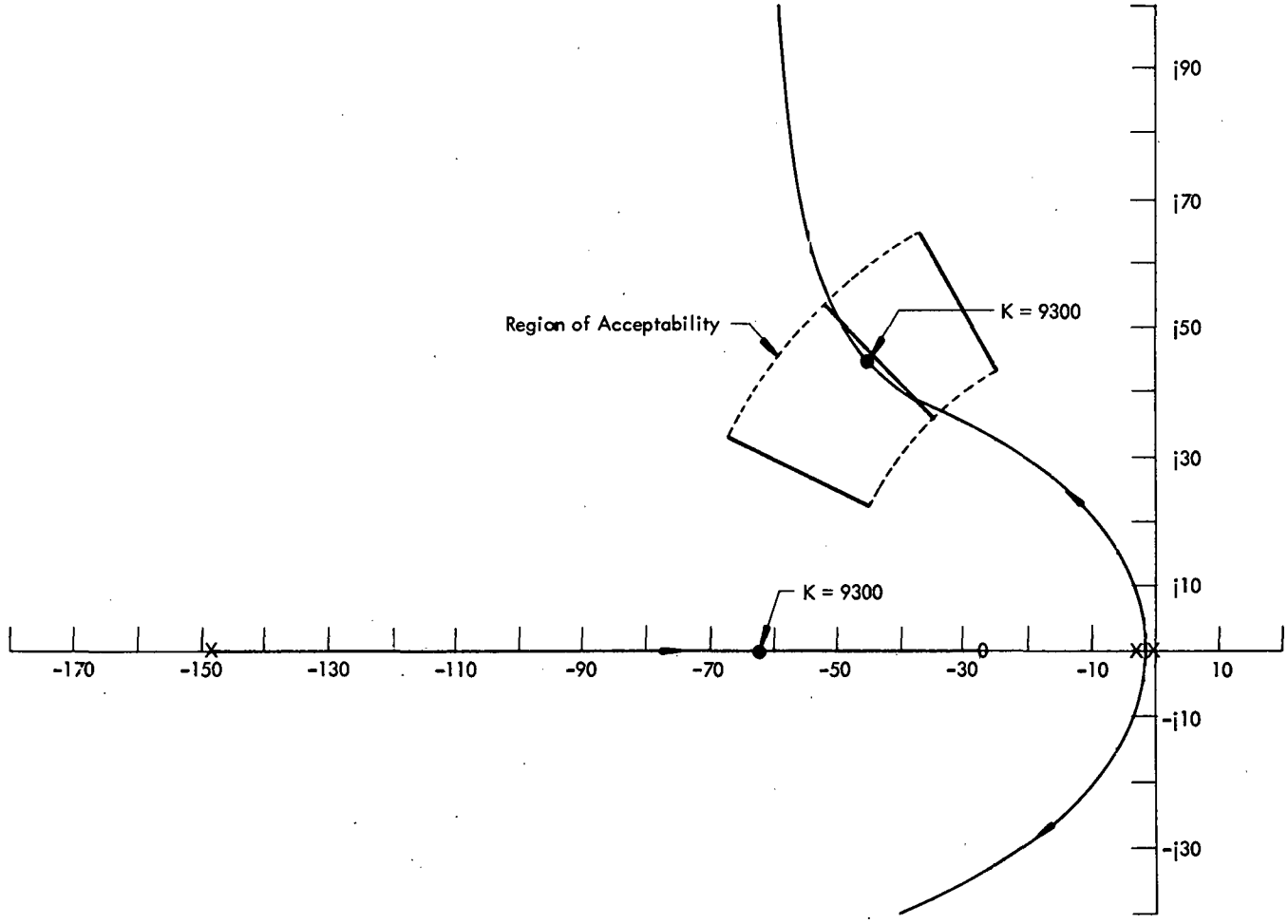

FIGURE 26

ROOT LOCUS OF SYSTEM UTILIZING LEAD COMPENSATION

$$E_v = \frac{1}{K_v} = \frac{1}{\lim_{s\to 0} \frac{s\,9300\,(s+27)}{s\,(s+2.6)(s+149)}}, \text{ or} \tag{94}$$

$$= \frac{(2.6)(149)}{(9300)(27)}, \text{ or}$$

$$= 0.000154 \text{ in/in/sec.}$$

In terms of minutes:

$$= \frac{0.000154}{60}, \text{ or}$$

$$= 0.0000257 \text{ in/in/min.}$$

This is almost, but not quite, within the design specifications.

Let us, therefore, insert a lag network in the system with a pole at $s = -1$ and a zero at $s = -2.5$. The closed-loop transfer function then becomes:

$$\frac{C(s)}{R(s)} = \frac{\frac{K_t\,(s+27)(s+2.5)}{s\,(s+2.6)(s+149)(s+1)}}{1 + \frac{K_t\,(s+27)(s+2.5)}{s\,(s+2.6)(s+149)(s+1)}}, \text{ or} \tag{95}$$

$$= \frac{K_t\,(s+27)(s+2.5)}{s^4 + 152.6\,s^3 + (439 + K_t)\,s^2 + (287.4 + 29.5\,K_t\,s) + 67.5\,K_t}.$$

The root locus of this system is shown in Figure 27 and passes well within the region of acceptability, and it has a root very near the design center of the system. These dominant complex roots lie at $s = -42 \pm j\,45$ which corresponds to a damping ratio of $\zeta = 0.68$ and an undamped natural frequency of $\omega_n = 61$ radians per second.

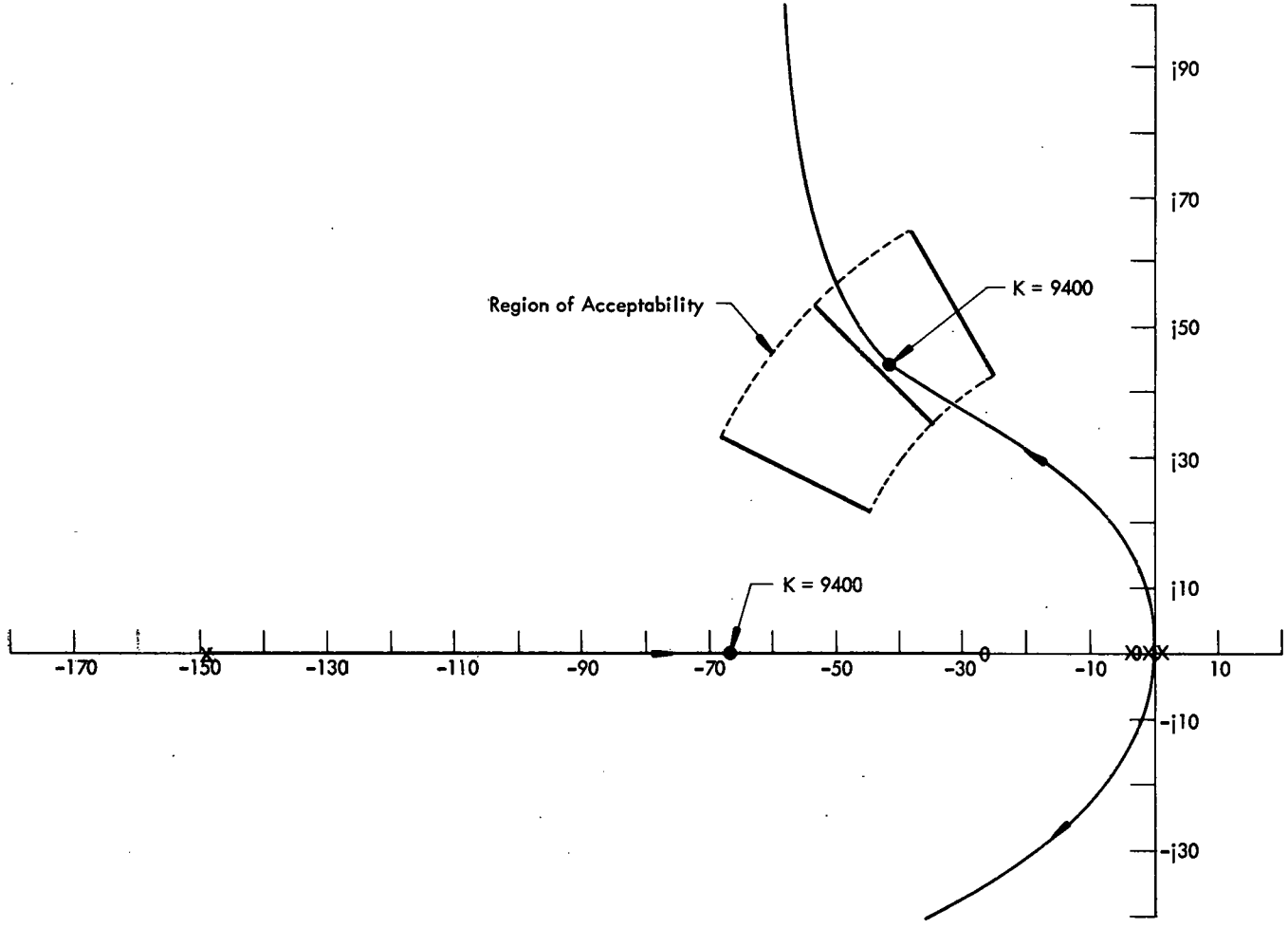

FIGURE 27

ROOT LOCUS OF THE FINAL SYSTEM

Since the damping ratio and the undamped natural frequency are within the region of acceptability, let us examine the velocity error which is given by:

$$E_v = \frac{1}{K_v} = \frac{1}{\lim_{s \to 0} s \frac{9400\,(s + 27)(s + 2.5)}{s\,(s + 2.6)(s + 149)(s + 1)}}, \text{ or} \tag{96}$$

$$= \frac{(2.6)(149)}{(9400)(27)(2.5)}, \text{ or}$$

$$= 0.00061 \text{ in/in/sec.}$$

In terms of minutes:

$$= \frac{0.00061}{60}, \text{ or}$$

$$= 0.0000102 \text{ in/in/min.}$$

We have, therefore, designed a system with the following characteristics:

ω_n = 61 radians per second,

ζ = 0.68, and

E_v = 0.000010 inch per inch per minute.

All of these values meet the design specification.

Final System

Experimental Results. The transfer function of the closed loop system is given by:

$$\frac{C\,(s)}{R\,(s)} = \frac{9400\,(s + 27)(s + 2.5)}{(s + 2.5)(s + 67)(s + 42 + j45)(s + 42 - j45)}. \tag{97}$$

The response of this system to an input step function is shown in Figure 28. This response has the following characteristics:

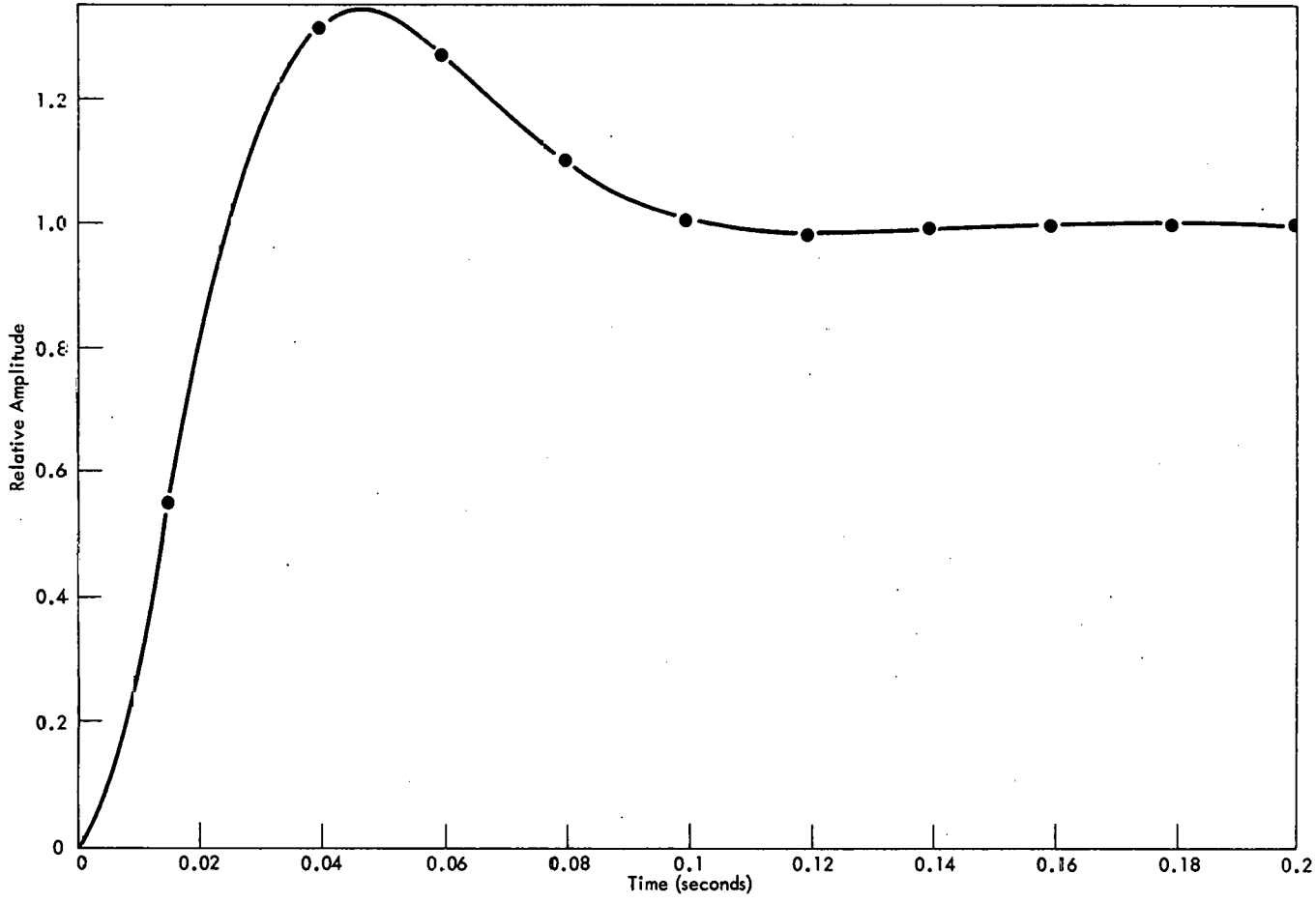

FIGURE 28

CALCULATED RESPONSE OF FINAL ACCELERATION SWITCHING VALVE SYSTEM TO AN INPUT STEP FUNCTION

Peak Time - 0.048 second,

Settling Time - 0.095 second, and

Percent Overshoot - 34.5%.

Samples of the response of the system to an input step function are shown in Figure 29. The characteristics of these samples are tabulated in Table II and compare relatively well with the calculated response. It should be noted that the response of the actual system is not as smooth as the calculated response. This discrepancy is due to many factors among which are noise and vibration.

Another reason that the response is not smooth is unique to the acceleration switching valve. In other words, it is due to the switching action of the valve. As may be seen, the output amplitude due to the switching action is approximately four to five per cent of the total displacement in this case. Of course this amplitude variation is constant no matter what the total displacement.

Discussion. The system has been designed utilizing both parallel and series compensation. Series compensation has been chosen because of the practical consideration discussed in Series Compensation, Page 74. It should be noted that the use of parallel compensation would require more components than series compensation in this case. Therefore, economics may be added to the reasons for choosing series compensation.

Comparing the calculated and actual responses shown in Figures 28 and 29 shows that there is relatively good agreement between the two. Note, however, that the actual response varies somewhat between any two inputs. Since the input

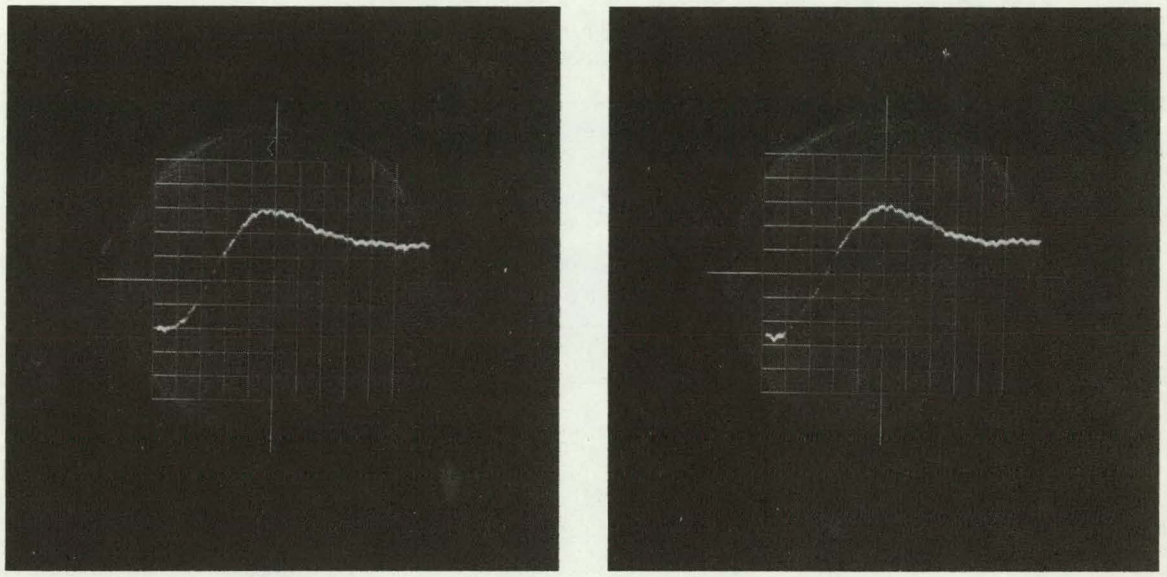

(a) (b)

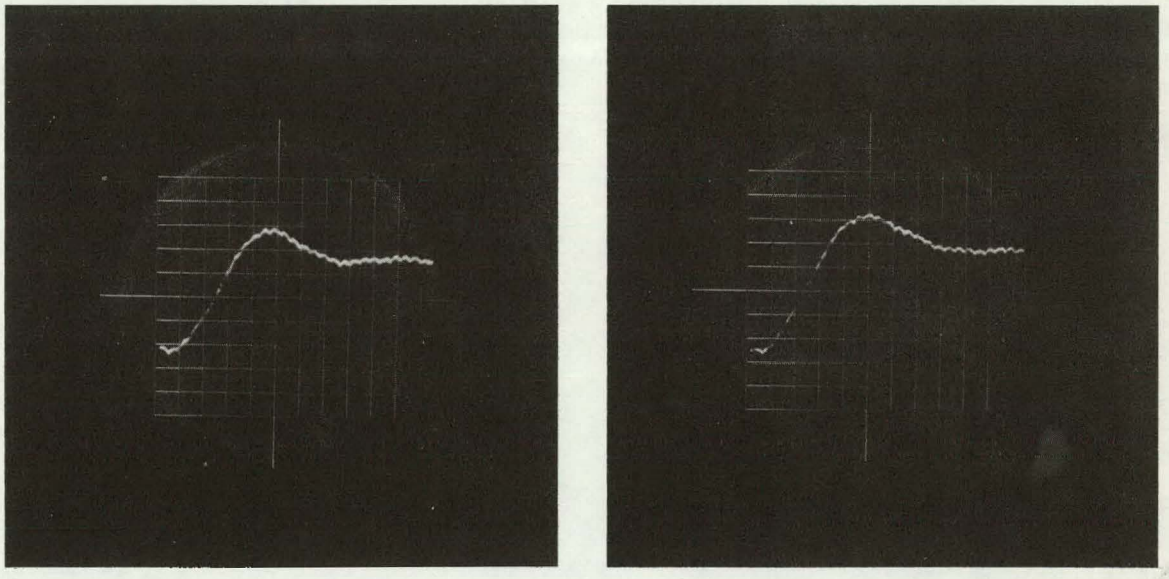

(c) (d)

FIGURE 29

SAMPLES OF RESPONSE TO AN INPUT STEP FUNCTION (TIME SCALE IS 10 MILLISECONDS PER SCALE DIVISION)

TABLE II

RESPONSE OF FINAL ACCELERATION SWITCHING VALVE SYSTEM TO AN INPUT STEP FUNCTION OF DISPLACEMENT

Response	Peak Time (Second)	Per Cent Overshoot	Settling Time (Seconds)
32-a	0.048	36	110
32-b	0.050	35	105
32-c	0.046	32	100
32-d	0.050	33	105

was maintained at a constant level, this can only be due to noise, disturbance, and/or some variation in the system characteristics.

The response of the system to the switching frequency must be considered in highly precision applications. This effect would be greatly reduced when controlling more massive actuators used in this system. It should be noted that this includes the majority of machine tools since the slide used in this system is relatively light when compared to the general market in machine tools.

Referring to Equation 67 (Chapter III, Page 45) we note that there are poles located at $s = -140 \pm j9000$. It was assumed that these frequencies were well above the spectrum of the system. These poles are due to leakage, the bulk modulus of the fluid, and the lapping characteristics of the valve. The leakage flow and the lapping characteristics of the valve are not likely to change substantially, but it is not uncommon for air and other contamination to collect in hydraulic fluids. These factors do not necessarily affect the fluid in a linear manner, but the macroscopic effect on the fluid may be approximated by a decreasing bulk modulus of the fluid.

To illustrate the possible effect of air in the fluid on the system, consider the original system with a pair of extraneous poles at $s = -180$. The open loop transfer function is then given by:

$$KG(s) = \frac{K_t (s + 2.5)(s + 27)}{s (s + 1)(s + 2.6)(s + 149)(s + 180)^2}, \tag{98}$$

and the transfer function of the closed loop system is given by

$$\frac{C(s)}{R(s)} = \frac{K_t (s + 2.5)(s + 27)}{s(s + 1)(s + 2.6)(s + 149)(s + 180)^2 + K_t (s + 2.5)(s + 27)}. \quad (99)$$

The root locus of this system is shown in Figure 30. The locus of this system is very far removed from the region of acceptability. It is, in fact, little better than the uncompensated system shown in Figure 19 (Page 61). The greatest damping ratio this system attains for any value of gain is $\zeta = 0.23$, and the system is obviously unacceptable.

It is a matter of practical interest that great care must be taken to insure that the system does not absorb air. It should be noted that the presence of air in the hydraulic systems may also have substantial nonlinear effects.

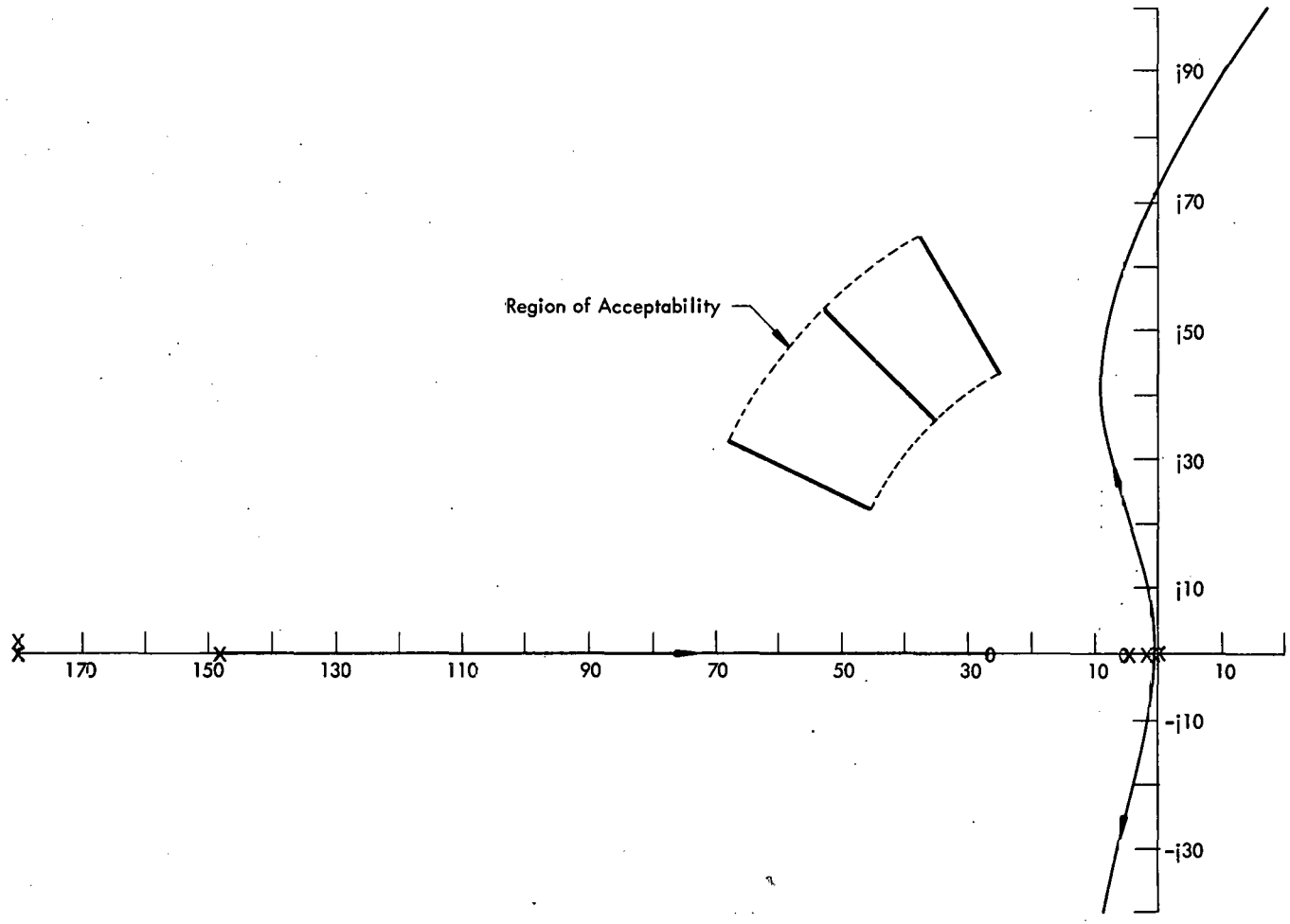

FIGURE 30

ROOT LOCUS OF SYSTEM WITH TWO EXTRANEOUS POLES

CHAPTER VI

CONCLUSION

In the choice of control elements for a given system, more often than not practical considerations are the determining factor. In this respect a possible disadvantage to the acceleration switching valve is its output variation at the switching frequency. In addition, the complexity of the electronic system relative to more conventional valves decreases the reliability of the system. This, however, may be more than offset by the increased reliability of the acceleration switching valve itself. Another practical advantage of the acceleration switching valve is the ease in which system balance may be accomplished. This advantage is due, primarily, to the fact that there is no necessity for mechanical adjustment of the acceleration switching valve.

In the design of the system, such important practical effects as system noise and nonlinearities were not rigorously considered. An attempt was made to restrict these effects by a choice of system design criteria. The acceleration switching valve has negligible dead band, and its response is more linear than more conventional control valves. Of course, saturation is important; however, due to the manner in which a machine tool operates, the error is never great. Saturation, therefore, is not as important in machine tool applications as in some other applications.

Electrohydraulic control systems may be designed by utilizing basic hydraulic concepts and judicial use of the technique of electrical analogies. By application of these techniques, the differential equation describing this system may be derived. By application of root-locus techniques with a knowledge of optimization procedures, systems with desirable transient responses and steady-state errors may be designed. In all cases, however, the design must be tempered with engineering judgment since the ultimate performance criterion of a machine tool control system is the quality of the parts it produces.

REFERENCES

REFERENCES

[1]Blackburn, John F., Gerhard Reethof, and J. Lowen Shearer, Fluid Power Control, John Wiley and Sons, Inc., New York, 1960.

[2]Binsfeld, John E. and Ray G. Spencer, "Measuring Electro-Hydraulic Systems," National Conference on Industrial Hydraulics, Vol. 13, 1959, pp. 51-59.

[3]Murtaugh, Stephen A., Jr., "An Introduction to the Time-Modulated Acceleration Switching Electrohydraulic Servomechanism," Journal of Basic Engineering, ASME, Paper No. 58-A-159.

[4]Moore, Morton E.,"The Acceleration Switching Valve Still Has Advantages," Control Engineering, June, 1960.

[5]Chubbuck, John G.,"Are High Performance and Low Cost Compatible in Hydraulic Servos?" Control Engineering, March, 1957.

[6]Truxal, John G., Control Engineers Handbook, McGraw-Hill Book Company, Inc., New York, 1958, pp. 15-17.

[7]Fuller, Dudley D., Theory and Practice of Lubrication for Engineers, John Wiley and Sons, Inc., New York, 1956, p. 19.

[8]Shearer, J. Lowen, "Dynamic Characteristics of Valve-Controlled Hydraulic Servomotors," ASME, Vol. 76, No. 6, 1954, pp. 895-903.

[9]Gaskell, Robert E., Engineering Mathematics, Henry Holt and Company, Inc., New York, 1958, p. 337.

[10]Sokolnikoff, I. S. and R. M. Redheffer, Mathematics of Physics and Modern Engineering, McGraw-Hill Book Company, Inc., New York, 1958.

[11]Lee, Shih-Ying and John F. Blackburn, "Contributions to Hydraulic Control - I. Steady-State Axial Forces on Control-Valve Pistons," Trans. ASME, 1952, pp. 1005-1016.

[12]Lamb, Sir Horace, Hydrodynamics, Dover Publications, New York, 1945.

[13]Pai, Shih-I, Viscous Flow Theory, I. Laminar Flow, D. Van Nostrand Company, Inc., Princeton, New Jersey, 1956.

[14]Bird, R. Byron, Warren E. Stewart, and Edwin N. Lightfoot, Transport Phenomena, John Wiley and Sons, Inc., New York, 1960.

[15]Seamone, W., Design and Performance Criteria of the Acceleration Switching Hydraulic Servo, Johns Hopkins University, Applied Physics Laboratory, APL/JHU CF-2653, June 19, 1957.

[16]Duncan, William J., A. S. Thom, and A. P. Young, An Elementary Treatise on the Mechanics of Fluids, Edward Arnold, Ltd., London, 1960.

[17]Dutcher, John L., "Position Regulators for Machine Tools," Machinery, The Industrial Press, New York, November, 1959, pp. 151-162.

[18]Graham, Dunstan and R. C. Lathrop, "The Synthesis of 'Optimum' Transient Response: Criteria and Standard Forms," Trans. AIEE, Vol. 72, Pt. II, pp. 273-288, November, 1953.

[19]Golinsky, Martin, An Analytical Determination of the Existence of Optimum Points in a Class of Networks, Institute of Science and Technology, The University of Michigan, Ann Arbor, Michigan, August, 1962, pp. 1-20.

[20]D'Azzo, John J. and Constantine H. Houpis, Feedback Control System Analysis and Synthesis, McGraw-Hill Book Company, Inc., New York, 1960.

[21]Schultz, W. C. and V. C. Rideout, "The Selection and Use of Servo Performance Criteria," Trans. AIEE, Pt. II, pp. 383-388, January, 1958.

[22]Truxal, John G., Automatic Feedback Control System Synthesis, McGraw-Hill Book Company, Inc., New York, 1955.

[23]Savant, C. J., Jr., Basic Feedback Control System Design, McGraw-Hill Book Company, Inc., New York, 1958.

APPENDIX A

TRANSFER FUNCTION MEASUREMENT

The circuit configuration for the measurement of the acceleration switching valve and hydrostatic slide transfer function was similar to the unity feedback system shown in Figure 31. Measurements were taken with no input (R (s) = 0); rather, the input for experimental determination is I(s). Two separate measurements were taken for a single input. These measurements were taken at Points (a) and (b).

With no input (R(s) = 0) we have:

$$\frac{C(s)}{I(s)} = \frac{KG(s)}{1 + H(s)\,KG(s)}. \tag{100}$$

Now, let

$$KG(s) = \frac{Z(s)}{P(s)} \text{ and} \tag{101}$$

$$H(s) = \frac{N(s)}{D(s)}. \tag{102}$$

Therefore, Equation 100 becomes:

$$\frac{C(s)}{I(s)} = \frac{K\,\frac{Z(s)}{P(s)}}{1 + \frac{N(s)}{D(s)}\,K\,\frac{Z(s)}{P(s)}}, \text{ or} \tag{103}$$

$$= \frac{K\,\frac{Z(s)}{P(s)}}{\frac{D(s)\,P(s) + K\,N(s)\,Z(s)}{D(s)\,P(s)}}, \text{ or}$$

$$= \frac{K\,Z(s)\,D(s)}{D(s)\,P(s) + K\,N(s)\,Z(s)}.$$

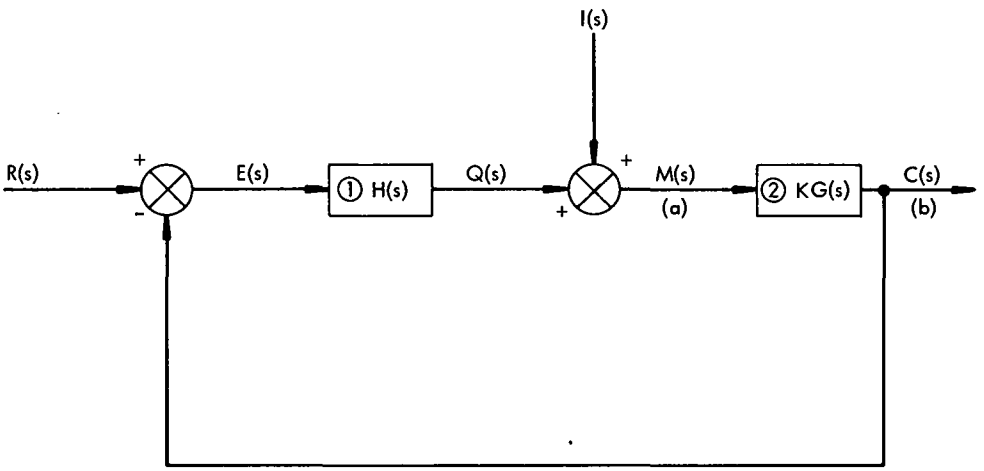

FIGURE 31

EXPERIMENTAL CONFIGURATION FOR TRANSFER FUNCTION DETERMINATION

The error is given by:

$$E(s) = R(s) - C(s), \text{ or} \tag{104}$$

$$= -C(s).$$

And, also:

$$M(s) = I(s) + Q(s), \text{ and} \tag{105}$$

$$Q(s) = H(s)\,E(s). \tag{106}$$

Substituting Equation 106 into Equation 105, we have:

$$M(s) = I(s) + H(s)\,E(s). \tag{107}$$

And, substituting Equation 104 into Equation 107, we have:

$$M(s) = I - H(s)\,C(s). \tag{108}$$

Dividing Equation 108 by I(s) yields:

$$\frac{M(s)}{I(s)} = 1 - H(s)\,\frac{C(s)}{I(s)}. \tag{109}$$

Now, substituting Equation 103 into Equation 109, we have:

$$\frac{M(s)}{I(s)} = 1 - \frac{N(s)}{D(s)}\,\frac{K\,Z(s)\,D(s)}{D(s)\,P(s) + K\,N(s)\,Z(s)}, \text{ or} \tag{110}$$

$$= \frac{D(s)\,P(s) + K\,N(s)\,Z(s) - K\,N(s)\,Z(s)}{D(s)\,P(s) + K\,N(s)\,Z(s)}, \text{ or}$$

$$= \frac{D(s)\,P(s)}{D(s)\,P(s) + K\,N(s)\,Z(s)}.$$

A measurement taken at Point (a) yields the relationship of Equation 110, and a measurement taken at Point (b) results in the relationship of Equation 103.

Now, dividing Equation 103 by Equation 110, we have:

$$\frac{\frac{C(s)}{I(s)}}{\frac{M(s)}{I(s)}} = \frac{\frac{K Z(s) D(s)}{D(s) P(s) + K N(s) Z(s)}}{\frac{D(s) P(s)}{D(s) P(s) + K N(s) Z(s)}}, \text{ or} \tag{111}$$

$$\frac{C(s)}{M(s)} = K \frac{Z(s)}{P(s)} = KG(s). \tag{112}$$

Equation 112 is the transfer function of Block 2 in Figure 31. Therefore, the transfer function of any element may be determined by making separate measurements at the input and output of the element with the system operating in a closed-loop condition.

This was the experimental method used in determining the transfer function of the acceleration switching valve and hydrostatic slide combination. Measurements were taken of the input to the acceleration switching valve and of the slide output position. The transfer function was then determined by Equation 112 where M(s) is the acceleration switching valve input, C(s) is the slide output position, and I(s) is the instrumentation input to the system.

It was necessary to use this procedure rather than the more straightforward measurement of input and output in an open-loop condition because it is very difficult to balance the acceleration switching valve and actuator in this condition. This is normally true of electrohydraulic systems with limited range.

APPENDIX B

COMPUTER PROGRAMS

Calculation of Characteristics Curves of the First Stage Hydraulic Amplifier

This program calculates points from Equations 27, 32, and 35 which are:

$$P_m = P_1 - P_4, \tag{27}$$

$$P_1 + (1 - M)\frac{A_1\sqrt{P_1}}{C_D A_2^2\sqrt{\frac{2}{\rho}}} Q_m + (1 - M)^2 \frac{A_1^2 P_1}{4A_2^2} = P_s - \frac{Q_m^2}{g_2^2}, \text{ and} \tag{32}$$

$$P_4 - (1 + M)\frac{A_4\sqrt{P_4}}{C_D A_3^2\sqrt{\frac{2}{\rho}}} Q_m + (1 + M)^2 \frac{A_4^2 P_4}{4A_2^2} = P_s - \frac{Q_m^2}{g_3^2}, \tag{35}$$

so that the family of $P_m - Q_m$ curves may be plotted. The flow chart for the program is shown in Figure 32.

Calculation of Root Loci

This program utilizes Share Program C2 C1 AEQ1 (SDA No. 223)[a] which calculates the n roots of the polynomial:

$$F(s) = a_n s^n + a_{n-1} s^{n-1} + a_{n-2} s^{n-2} + \ldots + a_1 s + a_o, \tag{113}$$

by the Newton-Raphson method as explained below. The coefficients a_o, a_1, ---, a_n are assigned initial values corresponding to a system gain of $K = 0$. This program has been modified by a calling sequence to increment the gain until large

---

[a]Share Distribution Agency, Program Distribution Center, IBM Corporation, 112 E. Post Road, White Plains, New York.

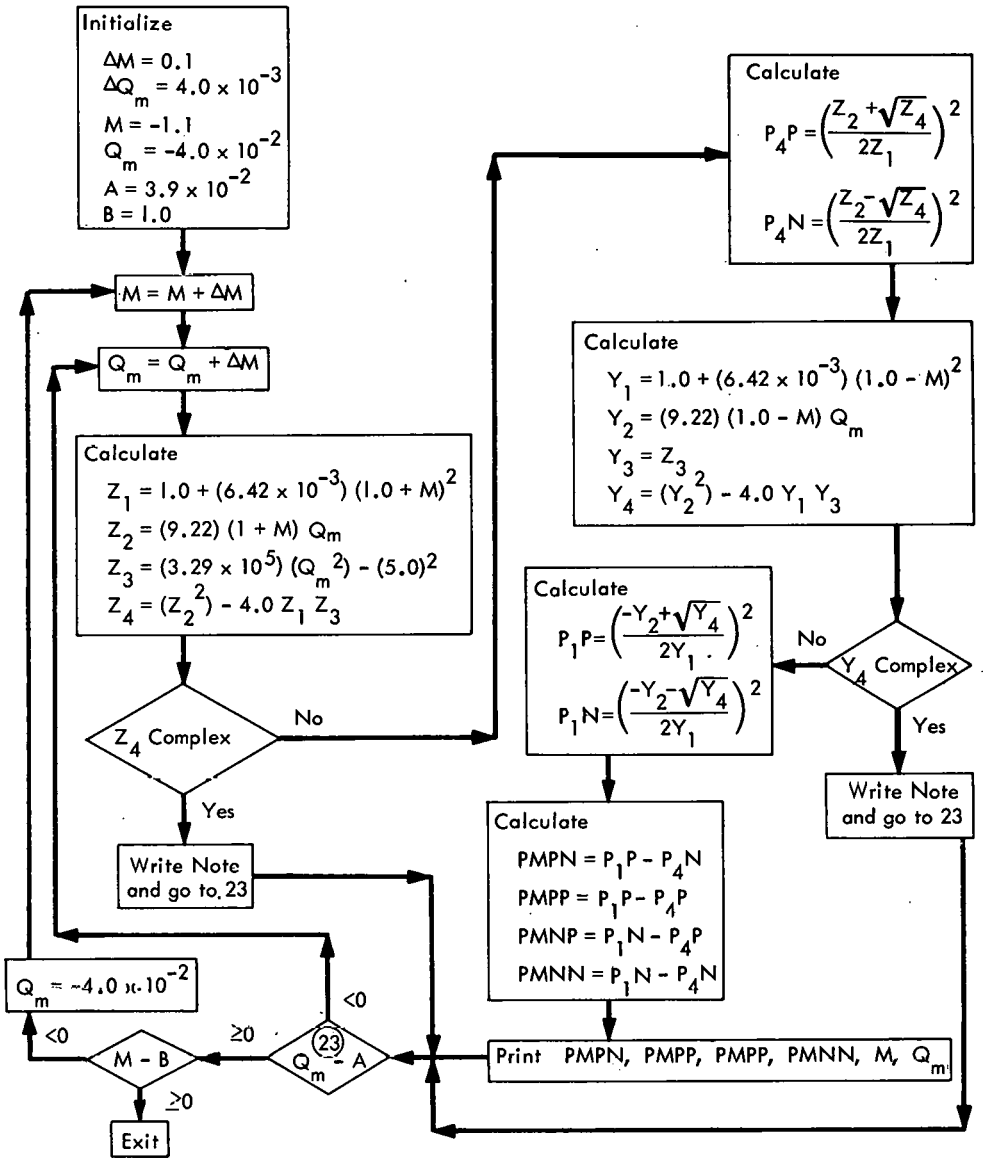

FIGURE 32

FLOW CHART FOR COMPUTER CALCULATION OF FIRST-STAGE HYDRAULIC AMPLIFIER CHARACTERISTIC CURVES

values of gain are approached. This modification results in a set of points describing the system root locus.

The program supplies the first estimate of a root, and the routine obtains better estimates by a series of iterations. When the root has converged to at least four octal figures, the polynomial is reduced to a polynomial of one degree less, and the process is repeated until all the roots are found.

If x_i^K is the K^{th} estimate of the i^{th} root, the routine uses the Newton-Raphson method for finding the next best estimate, x_i^{K+1}. This method consists of iterations on the formula:

$$x_i^{K+1} = x_i^K - \frac{F(x_i^K)}{F'(x_i^K)}, \tag{114}$$

where F' means the first derivative of F.

Calculation of Time Response

This program utilizes Share Program C3XML CL1Z (SDA No. 1125)[b] to determine the inverse Laplace transform. If the transfer function of a system is given by:

$$F(s) = \frac{K \prod_{i=1}^{n} (s - s_i)}{K \prod_{i=1}^{m_1} (s - s_i)}, \tag{115}$$

[b] Ibid.

where s_i and s_l are the zeros and poles, respectively, of the transfer function, then the coefficients and time response of the inverse transform is computed by the Heaviside expansion.[c]

The inverse transform is printed out in the following form:

Real root, $(s + a)$

$$C \epsilon^{-at}$$

Double root, $(s + a)^2$

$$(C_1 + C_2 t) \epsilon^{-at}$$

Triple root, $(s + a)^3$

$$(C_1 + C_2 t + C_3 t^2) \epsilon^{-at}$$

Complex conjugate roots, $(s + a + jb)(s + a - jb)$

$$C_1 \cos(bt + \theta) \epsilon^{-at}$$

The time response is printed as follows:

TIME-DISPLACEMENT-VELOCITY-ACCELERATION

where:

---

[c]Stanford Goldman, Transformation Calculus and Electrical Transients, Prentice-Hall, Inc., Englewood Cliffs, New Jersey, 1949.

DISPLACEMENT $= F^{-1}(s)$,

VELOCITY $= \dot{F}^{-1}(s)$, and

ACCELERATION $= \ddot{F}^{-1}(s)$.

APPENDIX C

MECHANIZATION OF INDICES OF PERFORMANCE[21]

Consider the generalized index of performance given by:

$$I = \int_0^\infty F\,[e\,(t),\ t\,]\,dt. \tag{116}$$

This function may be evaluated by the generalized analog computer configuration shown in Figure 33. The method of synthesis by this method may be summarized by the following procedure:

1. Adjust the function generator for the proper performance criterion.
2. Apply r (t) and obtain c (t) = r (t) - e (t).
3. Form F [e (t), t].
4. Integrate F [e (t), t] to obtain I.
5. Adjust the system for minimum I.

Neither the system nor the index of performance is necessarily linear. It is limited only by the analog computer and the function generator.

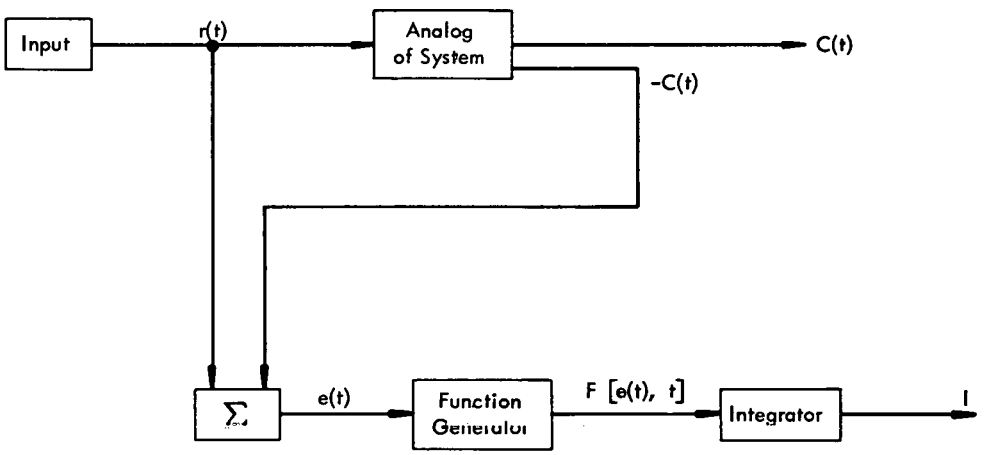

FIGURE 33

ANALOG COMPUTER MECHANIZATION OF

INDICES OF PERFORMANCE

TABLE OF SYMBOLS

Symbol	Meaning	Value	Units
A_A	Load Surface Area	126	$inches^2$
A_C	Spool Surface Area	$A_1 + A_2$	
A_1	Surface Area of Lands	0.321	$inch^2$
A_2	Connecting Rod Surface Area	0.339	$inch^2$
A_L	Area of Load Piston	5.86	$inches^2$
A_m	Area of Spool Piston Face	0.0314	$inch^2$
A_N	Area of Nozzle	0.0000785	$inch^2$
A_o	Area of Orifice	0.0000126	$inch^2$
β	Bulk Modulus of Fluid	2.5×10^5	lb/in^2
C_D	Coefficient of Discharge	0.6	
C_L	Actuator Stiffness Coefficient	0.00	$in^3/sec/lb/in^2$
C_m	Stiffness Sensitivity	-2.4×10^{-4}	$in^3/sec/lb/in^2$
C (t)	Output Position		inches
d_c	Diameter of Pressure Outlet	0.05	inch
D_o	Diameter of Inlet Orifice	0.0050	inch
D_N	Diameter of Nozzle	0.0020	inch
f_L	Viscous Friction Coefficient of the Load		
h_L	Radial Clearance Between Load and Bushing	0.002	inch

Symbol	Meaning	Valve	Units
h_1	Radial Clearance Between Spool Lands and Bushing	0.0001	inch
h_2	Radial Clearance Between Connecting Rods and Bushing	0.03	inch
KG(s)	Transfer Function of the Acceleration Switching Valve and Hydrostatic Slide		in/sec/UNB
K_L	Actuator Flow Sensitivity	880	$in^3/sec/in$
K_m	Spool Flow Sensitivity	3.0×10^{-3}	$in^3/sec/UNB$
K_v	Velocity Error Constant		in/sec/in
L_c	Length of Control Chamber	0.25	inch
L_m	Algebraic Sum of Damping Lengths	0.000	inch
L_t	Length of Tubing in Valve (from inlet to one control chamber)	1.9	inch
M_L	Mass of Load	0.141	$lb\text{-}sec^2/in$
M_m	Mass of Spool	2.0×10^{-4}	$lb\text{-}sec^2/in$
m (t)	Modulation Index	$\frac{T_1 - T_2}{T_1 + T_2}$	% UNB
μ	Viscosity	3.7×10^{-6}	$lb\text{-}sec/in^2$
P_D	Pressure Drop Across Second Stage Orifice		lb/in^2
P_m	Load Pressure in First Stage		lb/in^2
P_L	Load Pressure in Second Stage		lb/in^2
P_s	Supply Pressure	500	lb/in^2

Symbol	Meaning	Value	Units
ρ	Mass Density of Hydraulic Fluid	7.95×10^{-5}	$lb\text{-}sec^2/in^4$
Q_L	Load Flow in Second Stage		in^3/sec
Q_{l_L}	Leakage Flow Around the Load		in^3/sec
Q_{l_m}	Leakage Flow Around the Spool		in^3/sec
Q_m	Load Flow in First Stage		in^3/sec
r_c	Radius of Control Chamber	0.125	inch
r_m	Radius of Spool	0.1	inch
r_t	Radius of Tubing	0.06	inch
$r(t)$	Input to System		inch
T_1	Period of Positive Cycle		second
T_2	Period of Negative Cycle		second
θ	Angle of Flow Entry	69	degrees
V_{i_L}	One-Half Volume of Entrained Fluid in Second Stage	16.5	$inch^3$
V_{i_m}	One-Half Volume of Entrained Fluid in First Stage	2.94×10^{-2}	$inch^3$
V_m	Volume of Spool	0.0234	$inch^3$
ω_n	Undamped Natural Frequency		radians/sec
$x(t)$	Spool Position		inches
x_{max}	Maximum Travel of Spool	0.03	inch
$y(t)$	Load Position		inches
ζ	Damping Ratio		